

# WORLDSIMBENCH: TOWARDS VIDEO GENERATION MODELS AS WORLD SIMULATORS

Anonymous authors

Paper under double-blind review

## ABSTRACT

Recent advancements in predictive models have demonstrated exceptional capabilities in predicting the future state of objects and scenes. However, the lack of categorization based on inherent characteristics continues to hinder the progress of predictive model development. Additionally, existing benchmarks are unable to effectively evaluate higher-capability, highly embodied predictive models from an embodied perspective. In this work, we classify the functionalities of predictive models into a hierarchy and take the first step in evaluating World Simulators by proposing a dual evaluation framework called WorldSimBench. WorldSimBench includes **Explicit Perceptual Evaluation** and **Implicit Manipulative Evaluation**, encompassing human preference assessments from the visual perspective and action-level evaluations in embodied tasks, covering three representative embodied scenarios: **Open-Ended Embodied Environment**, **Autonomous Driving**, and **Robot Manipulation**. In the Explicit Perceptual Evaluation, we introduce the HF-Embodied Dataset, a video assessment dataset based on fine-grained human feedback, which we use to train a Human Preference Evaluator that aligns with human perception and explicitly assesses the visual fidelity of World Simulators. In the Implicit Manipulative Evaluation, we assess the video-action consistency of World Simulators by evaluating whether the generated situation-aware video can be accurately translated into the correct control signals in dynamic environments. Our comprehensive evaluation offers key insights that can drive further innovation in video generation models, positioning World Simulators as a pivotal advancement toward embodied artificial intelligence.

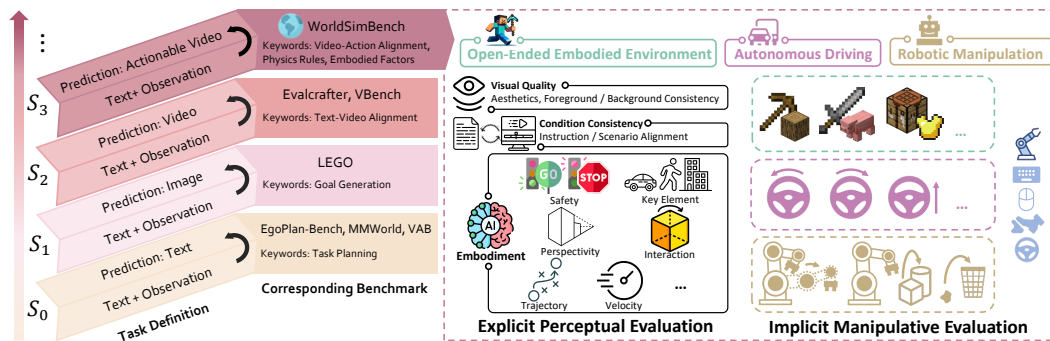


Figure 1: **Overview of the hierarchical capabilities of the Predictive Models.** Models at higher stages demonstrate more advanced capabilities. We take the initial step in evaluating Predictive Generative Models up to the  $S_3$  stage, known as World Simulators, by introducing a parallel evaluation framework, WorldSimBench. WorldSimBench assesses the models both Explicit Perceptual Evaluation and Implicit Manipulative Evaluation, focusing on video generation and action transformation across three critical embodied scenarios.

Table 1: **Comparisons between existing Predictive Model benchmarks.** Interactive Environment refers to the interaction with the simulation environment during the prediction phase. Task-Level Interaction denotes that each task interacts once, whereas Action-Level Interaction represents the frequency of interactions that occur through the generation of actions for control purposes.

Benchmark	Input Modality	Output Modality	Based Method	Stage	Interactive Env.	Evaluation Strategy
AgentBench (Liu et al., 2023b)	Text	Text	LLM	$S_0$	Task-Level	Human Judgement
EgoPlan-Bench (Chen et al., 2023)	Text & Images	Text	MLLM	$S_0$	N/A	Multi-choice
MMWorld (He et al., 2024)	Text & Images	Text	MLLM	$S_0$	N/A	GPT Judgement
VAB (Liu et al., 2024a)	Text & Images	Text	MLLM	$S_0$	Task-Level	Human Judgement
LEGO (Lai et al., 2023)	Text & Images	Image	IGM	$S_1$	Task-Level	Feature Similarity
VBench (Huang et al., 2024)	Text	Video	VGM	$S_2$	N/A	Feature Similarity
EvalCrafter (Liu et al., 2024b)	Text & Images	Video	VGM	$S_2$	N/A	Feature Similarity
WorldSimBench	Text & Images	Actionable Video	VGM	$S_3$	Action-Level	Human Preference Evaluator Embodied Metric

## 1 INTRODUCTION

Before taking action, humans make predictions based on their objectives and observations of the current environment. These predictions manifest in various forms, *e.g.*, textual planning, visual imagination of future scene changes, or even subconscious planning at the action level. With the development of generative models, agents driven by these models are exhibiting predictive capabilities that enable them to complete embodied tasks by making human-like predictions, *e.g.*, high-level planning (Driess et al., 2023; Li et al., 2024), image-based guidance (Lai et al., 2023; Black et al., 2023), or future video prediction to drive actions (Du et al., 2023; 2024)). We refer to these models as **Predictive Models**. Recently, these models have been widely applied across various domains spanning from developing agents to solve inference tasks to leveraging predictions for driving robots to perform specific actions.

Nevertheless, the rich application scenarios and diverse model designs make predictive models a broad family. However, without categorizing them based on their inherent characteristics, the advancement of predictive model development remains limited. This leads to our first question: *Can we establish a reasonable hierarchical system for Predictive Models based on their output modality?* With a well-defined categorization, *we can better target the evaluation of Predictive Models from different perspectives in diverse embodied environments*, ensuring that their strengths and weaknesses are adequately assessed. In the literature, existing evaluations have typically focused on task planning capabilities by assessing text outputs or evaluating visual outputs from an aesthetic perspective. However, such approaches significantly limit the evaluation of highly embodied Predictive Models, as embodied scenarios are more concerned with physical properties (*e.g.*, perspective consistency, object breakability), which these methods fail to effectively assess. This brings us to our second question: *Can we conduct a more detailed evaluation of highly embodied Predictive Models from an embodied perspective?*

To answer the first question, we categorize the functionalities of Predictive Models into a hierarchy from  $S_0$  to  $S_3$ , *defined by the model’s capabilities and output modality*, accompanied by corresponding evaluation benchmarks as illustrated in Fig. 1. *Models are classified based on the output modality in their output modalities.* From lower to higher stages, the models are capable of generating: text, images, videos, and actionable videos (*i.e.*, the videos that can be translated into actions). It is worth noting that Predictive Models at  $S_3$  capable of generating actionable videos integrate robust 3D scene understanding and physical rule priors to provide precise guidance for generating executable actions. These models are closely aligned with the recently proposed concept of World Simulators (Yang et al., 2023).

To answer the second question, we review the related benchmarks, as listed in Tab. 1. Evaluations on models in  $S_0$  that generate text primarily focus on assessing task planning capabilities, while  $S_1$  and  $S_2$  assessments on visual output measure aesthetic quality through feature similarity analyses with ground truth data. With clearly defined evaluation dimensions and extensive annotated datasets, both types of assessments can be effectively conducted. However, evaluating World Simulators introduces complexities due to the intricate physical definitions involved. Additionally, conventional evaluation methods are inadequate for assessing the actionability of the generated videos, as there is no definite ground truth for actionable videos towards completing a specific embodied task. These factors pose significant challenges to the evaluation of World Simulators.

We argue that an evaluation aligned with human perception could provide a more intuitive and accurate reflection of the characteristics of the synthesized videos, including their adherence to physical rules. Besides, the actionability can be assessed through a closed-loop manner in simulations deployed with a unified video-to-action policy network. Considering these aspects, we take the very first step in evaluating World Simulators by proposing a dual evaluation framework called WorldSimBench. As shown in Fig. 1, WorldSimBench assesses World Simulators through two complementary approaches: **Explicit Perceptual Evaluation**, which focuses on the Visual Quality, Condition consistency, and Embodiment of the generated content, and **Implicit Manipulative Evaluation**, which measures the World Simulator’s performance through the conversion of video into control signals. We present three representative embodied scenarios: **Open-Ended Embodied Environment (OE)**, **Autonomous Driving (AD)**, and **Robot Manipulation (RM)**, to thoroughly evaluate the capability of World Simulators in generating and representing scenario-specific attributes.

In the Explicit Perceptual Evaluation, we first define evaluation criteria which is used to construct a comprehensive set of prompts specific to each scenario. The prompt lists are then used by various video generation models to produce a large number of video clips. Following extensive human feedback and annotation, these video clips are compiled into the HF-Embodied dataset which consists of a total of 35,701 tuples with multi-dimensional scores and fine-grained human feedback. Additionally, we train Human Preference Evaluator, using the HF-Embodied dataset to assess World Simulators at the perceptual level, offering a robust evaluation of both their visual fidelity and contextual accuracy. For the Implicit Manipulative Evaluation, we deploy three simulation environments for the three embodied scenarios respectively. These environments are used to collect data and train inverse dynamic or goal-based video-to-action models capable of mapping future videos to actions. In each of these embodied scenarios, the World Simulator is tasked with generating situation-aware videos in real-time, based on current observations and provided text instructions. These generated videos are then converted into actions using the pre-trained video-to-action models. The effectiveness of the World Simulator is implicitly evaluated by measuring the performance of the tasks, using relevant metrics to reflect the quality and accuracy of the generated video.

In summary, the main contributions are as follows: (1) We categorize the functionalities of Predictive Models into a hierarchy, **defined by the model’s capabilities and output modality**, to advance research and development in the field and take the very first step in evaluating World Simulators. (2) We propose a dual evaluation framework called WorldSimBench, through Explicit Perceptual Evaluation and Implicit Manipulative Evaluation, we conducted a comprehensive evaluation of the World Simulator’s capabilities from an embodied perspective, focusing on both the visual and action levels. (3) We conducted extensive testing across multiple models and performed a thorough analysis of the experimental results. Our findings highlight the strengths and limitations of current World Simulators and provide actionable insights for improving future video generation models. (4) We developed HF-Embodied Dataset, which includes fine-grained human feedback across three scenarios and 20 dimensions, with a total of 35,701 entries. This dataset, containing both human ratings and the reasons behind them, not only enables the evaluation of World Simulators but also provides broader applications (*e.g.*, alignment) for future video generation models.

## 2 RELATED WORK

**Predictive Models.** Predictive models are capable of generating process representations that map the current state to future states by incorporating current state representations and control over future trends. Predictive Text Model, built on LLMs (Radford et al., 2019; Touvron et al., 2023; Chiang et al., 2023) and MLLMs (Achiam et al., 2023; Team et al., 2023; Liu et al., 2023a; Yin et al., 2023), generate future predictions in the text modality by accepting current state representations and text instructions. These models have demonstrated impressive performance in high-level planning tasks for embodied agents (Driess et al., 2023; Li et al., 2024; Qin et al., 2024; Chen et al., 2024; Zhang et al., 2024b; Lu et al., 2024). Similarly, image generation models (Brooks et al., 2023; Fu et al., 2023) as Predictive Image Model (Lai et al., 2023; Black et al., 2023; Zhou et al., 2024) can produce future goal images, showcasing strong capabilities during the decision-making phase of embodied agents. Predictive Video Model (Du et al., 2024, 2023), based on video generation models (Janner et al., 2022), have made some progress in embodied control. However, due to limitations in data or models, the generated videos often lack essential physical representations and logical consistency, restricting their applicability to fixed scenarios and single tasks.

With the advancement of diffusion transformer (Peebles & Xie, 2023) and the extensive utilization of large-scale internet video datasets (Bain et al., 2021; Ebert et al., 2021; Goyal et al., 2017; Grauman et al., 2022), certain Predictive Actionable Video Model (Yang et al., 2023) models, also known as World Simulators, have achieved more precise representations of physical laws and 3D environments.

**Evaluation of Predictive Models.** With the advancement of predictive models, research has also expanded to evaluate the capabilities of models at different stages. Liu et al. (2023b); Chen et al. (2023); Shi et al. (2024); Liu et al. (2024a) conducted text-level and task completion evaluations for Predictive Text Model at the  $S_0$  stage. Lai et al. (2023) performed score-based evaluations from an aesthetic perspective for Predictive Image Model at the  $S_1$  stage. Huang et al. (2024); Liu et al. (2024b) also assessed the aesthetic quality of videos generated by Predictive Video Model at the  $S_2$  stage. We take the first step in evaluating World Simulators through an embodied perspective.

### 3 PREDICTIVE MODEL CATEGORY DEFINITION

In this section, we concretely categorize predictive models based on the model’s capabilities and output modality. The detailed categorization stage of Fig. 1 is illustrated below,

- **Stage  $S_0$ :** At this stage, predictive models can generate corresponding predictions based on instructions and observations but are limited to textual modality. Benchmarks at this stage conduct text-level and task-completion evaluations through output text planning.
- **Stage  $S_1$ :** At this stage, predictive models can generate visual predictions based on instructions and observations, but without incorporating temporal information. Benchmarks at this stage conduct aesthetic evaluation for generated images.
- **Stage  $S_2$ :** At this stage, predictive models can generate corresponding video predictions based on both instructions and observations. Yet, due to limited model capabilities, the evaluation at this level focuses solely on the aesthetic quality of the generated outputs.
- **Stage  $S_3$ :** At this stage, predictive models can generate corresponding video predictions based on instructions and observations, with the predicted video content adhering to physical rules and aligning with the executed actions. These models are known as **World Simulators** (Ha & Schmidhuber, 2018; Yang et al., 2023), and WorldSimBench is a benchmark specifically designed to evaluate these World Simulators.

The rapidly evolving field of World Simulators offers exciting opportunities for advancing Artificial General Intelligence, with significant potential to enhance human productivity and creativity, especially in embodied intelligence. Therefore, conducting a comprehensive embodied evaluation of World Simulators is crucial.

### 4 WORLDSIMBENCH CONSTRUCTION

WorldSimBench evaluates the embodied capabilities of World Simulators across two distinct levels. The **Explicit Perceptual Evaluation** assesses the simulators based on human-perceived quality across different embodied scenarios, while the **Implicit Manipulative Evaluation** implicitly evaluates the simulators’ capabilities by converting the generated videos into control signals and observing their performance in various closed-loop embodied tasks.

The evaluation of World Simulators encompasses three critical embodied scenarios: **Open-Ended Embodied Environment (OE)**, **Autonomous Driving (AD)**, and **Robot Manipulation (RM)**. Minecraft serves as a popular testbed for **OE**, providing a challenging platform for agents to handle complex, unstructured tasks. In the context of **AD**, especially in outdoor settings, ensuring the stability and robustness of the agent’s actions is crucial, making it an essential domain for assessing a World Simulator’s capability in dynamic and uncertain environments. **RM**, a core task in embodied intelligence, demands precise and adaptive control, testing the world simulator’s ability to generate actionable predictions that align with physical interactions. Together, these scenarios provide a comprehensive benchmark for evaluating the effectiveness of World Simulators across a range of real-world tasks.

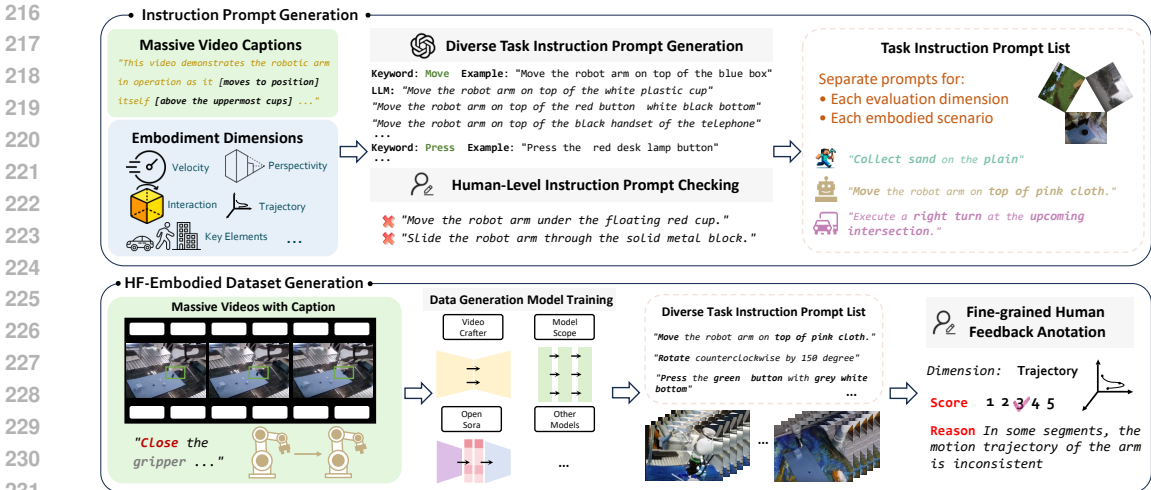


Figure 2: Overview of **Explicit Perceptual Evaluation**. (Top) **Instruction Prompt Generation**. We use a large collection of video captions from the internet and our predefined embodied evaluation dimensions. These are expanded using GPT and manually verified to create a corresponding Task Instruction Prompt List for data generation and evaluation. (Bottom) **HF-Embodied Dataset Generation**. Massive internet-sourced embodied videos with captions are used to train data generation models. Fine-grained Human Feedback Annotation is then applied to the embodied videos according to the corresponding Task Instruction Prompt List, covering multiple embodied dimensions.

#### 4.1 EXPLICIT PERCEPTUAL EVALUATION

In Explicit Perceptual Evaluation, we propose Hierarchical Evaluation Dimensions, based on which we build a video assessment dataset annotated through fine-grained human feedback, named HF-Embodied Dataset. The dataset is constructed based on three key resources, each corresponding to a specific embodied scenario: a curated dataset of Minecraft videos from the internet for **OE** (Baker et al., 2022), real-world driving data for **AD** (Caesar et al., 2020), and real-world robot manipulation videos annotated with text instructions for **RM** (Chen et al., 2024). Using HF-Embodied Dataset, we train a Human Preference Evaluator to perform perceptual evaluations of World Simulators.

##### 4.1.1 HIERARCHICAL EVALUATION DIMENSION

We develop a hierarchical evaluation dimension checklist for the three embodied scenarios, as illustrated in Tab. 2, which can be categorized into three main aspects: **Visual Quality**, **Condition Consistency**, and **Embodiment**. (1) Visual Quality primarily assesses the overall quality of video generation, including Aesthetics, Background and Foreground Consistency. (2) Condition Consistency focuses on the alignment with the input instruction. For tasks in **OE** that involve distinct scenarios, we additionally define Scenario Alignment to assess the alignment to the specific scenarios outlined in the instruction. (3) Embodiment has different definitions depending on the scenario. As all tasks require movement along a certain trajectory, we uniformly define Trajectory to evaluate the rationality of object movement in the video (e.g., whether a robotic arm avoids obstacles during motion). In **AD** and **RM**, we define Perspective to assess whether the video exhibits a clear sense of depth. In **OE** and **RM**, we define Embodied Interaction to evaluate the plausibility of interactions with objects. We also define Velocity in **OE** to determine whether speed varies appropriately across different environments (e.g., slower movement in water). In **AD**, we define Key Element to evaluate the rendering quality and consistency of crucial embodied elements, e.g., pedestrians. We also introduce Safety in **AD** to assess whether the embodied actions comply with traffic rules. More details in Sup. A.

##### 4.1.2 INSTRUCTION PROMPT GENERATION

Using the Hierarchical Evaluation Dimension and massive video captions from the key resources, we create a foundational but comprehensive prompt list. We utilize the knowledge of LLMs, *i.e.* ChatGPT, to extend the meta-prompts across a wide range. After manual screening for relevance, di-



Table 2: **Hierarchical Evaluation Dimension.** The dimensions are categorized into three main aspects: Visual Quality for evaluating the overall quality, Condition Consistency for evaluating the alignment to the input instruction, and Embodiment for evaluating embodied related factors like physical rules.

Embodied Scenarios	Visual Quality	Condition Consistency	Embodiment
Open-Ended Embodied Environment (OE)	Background Consistency (BC) Foreground Consistency (FC)	Instruction Alignment (IA) Scenario Alignment (SA)	Velocity (VC) Trajectory (TJ) Embodied Interaction (EI)
Autonomous Driving (AD)	Aesthetics (AE)	Instruction Alignment (IA)	Perspectivity (PV) Trajectory (TJ) Key Element (KE) Safety (SF)
Robot Manipulation (RM)	Aesthetics (AE) Background Consistency (BC) Foreground Consistency (FC)	Instruction Alignment (IA)	Perspectivity (PV) Trajectory (TJ) Embodied Interaction (EI)

versity, and data distribution, we compile the Task Instruction Prompt List, which separates prompts for each content-embodied scenario and each evaluation dimension, as shown in Fig. 2.

#### 4.1.3 HF-EMBODIED DATASET GENERATION

**Data Preparation.** We select multiple video generation models and train them using a large corpus of videos and corresponding captions from the key resources. Due to the capabilities of the open-source video generation model, we conduct targeted training for each of the three distinct embodied scenarios individually, thereby developing several data generation models for different embodied scenarios. These models are then used to produce a substantial amount of instruction-following embodied videos, based on the corresponding captions, and the initial image condition where applicable (first frame conditioned text-to-video to generate situation-aware videos).

**Human Annotation.** We use human annotation to label the generated videos. Based on the Hierarchical Evaluation Dimension, we establish specific annotation guidelines and numerous in-context examples for the annotators. For each dimension, annotators are instructed to score the video solely based on its performance within that particular dimension and provide corresponding reasoning. For instance in RM, as illustrated in Fig. 2, under the dimension of Trajectory, annotators are required to evaluate the video exclusively on the generation quality of the motion trajectory. They are instructed not to consider other elements (*e.g.*, the rendering quality of the robot arm) or other dimensions (*e.g.*, consistency with instructions). Additionally, annotators are asked to provide fine-grained feedback on any deficiencies, *e.g.*, “inconsistent trajectory”. As a result, we construct the HF-Embodied Dataset, which consists of a total of 35,701 tuples, each comprising a video, text instruction, multi-dimensional scores, and the potential reasons. More details in Sup. B.1.

#### 4.1.4 HUMAN PREFERENCE EVALUATOR

The objective is to develop a video scoring model that assesses videos across multiple dimensions aligning with human perception. The model takes a generated video and a prompt as input and outputs a score ranging from 1 to  $n$  ( $n$  is defined specifically for each embodied scenario). The prompt includes both the video generation instructions and an explanation of the evaluation criteria. Leveraging the strong video understanding capabilities of multimodal large language models, we fine-tune Flash-VStream (Zhang et al., 2024a), a VideoLLM, aligning it with human perception on HF-Embodied Dataset. Only LoRA (Hu et al., 2021) parameters are trained. This enables the model to effectively grasp the evaluation metrics for embodied tasks and produce accurate scores, while maintaining its video perception and reasoning ability. We prove the effectiveness and generalizability of our Human Preference Evaluator in Sec. 5.2.

#### 4.1.5 EVALUATION METRICS.

The evaluation of a video generation model is based on the scores assigned by the evaluator across various dimensions. For each dimension, the video generation model generates videos guided by several carefully selected instructions sourced from Task Instruction Prompt List that are strongly aligned with the specific evaluation criteria, *e.g.*, “explore on the beach” for Embodied Scenario in OE. The final metric for each model is computed as the average score across all dimensions. The evaluated dimensions for each embodied scenario are listed in Tab. 2.

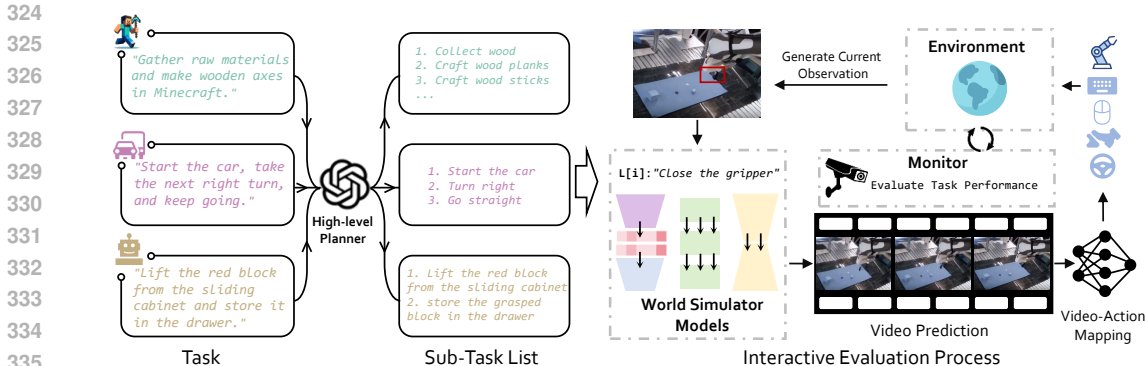


Figure 3: Overview of **Implicit Manipulative Evaluation**. Embodied tasks in different scenarios are decomposed into executable sub-tasks. The video generation model generates corresponding predicted videos based on the current instructions and real-time observations. Using a pre-trained IDM or a goal-based policy, the agent executes the generated sequence of actions. After a fixed timestep, the predicted video is refreshed by sampling again from the video generation model, and this process repeats. Finally, the success rates of various embodied tasks are obtained through monitors in the simulation environment.

## 4.2 IMPLICIT MANIPULATIVE EVALUATION

The Implicit Manipulative Evaluation assesses the capabilities of World Simulators across various embodied scenarios by treating the simulator as a low-level decision maker for situational contexts. Using pre-trained video-to-action models, we implicitly evaluate the performance of the World Simulators by observing their effectiveness in closed-loop embodied task tests.

### 4.2.1 SIMULATION CONSTRUCTION

The Implicit Manipulative Evaluation is conducted using the following three simulation platforms, for specific settings, please refer to the Supplementary Material.

**OE** We employ MineRL as the Minecraft simulator, with the observation space limited to RGB images and the action space confined to keyboard and mouse controls. We adopt the Steve-1 benchmarks (Lifshitz et al., 2024), with task descriptions *e.g.*, "chop a tree."

**AD** We conduct standard closed-loop evaluations using the CARLA (Dosovitskiy et al., 2017) simulator on the LangAuto Benchmark (Shao et al., 2024). Task descriptions include instructions like "do not deviate from this route."

**RM** We employ CALVIN (Mees et al., 2022) as the robot manipulation simulator, using only RGB images for the observation space and limiting the action space to the 7-DOF (degrees of freedom) of the robot arm. Task descriptions include commands *e.g.*, "pull the handle to open the drawer."

### 4.2.2 EMBODIED TASK EVALUATION

**Evaluation Pipeline.** As illustrated in Fig. 3, we first leverage existing or custom-trained video-to-action models as intermediaries between the World Simulator and the agent performing closed-loop tasks, for the selected benchmarks across three simulation environments. This approach enables the transformation of the predicted future videos from the World Simulator into executable control signals in real-time, thereby indirectly evaluating the World Simulator’s capability through the successful completion of embodied tasks. The evaluation process is tailored to the specific nature of the models under consideration, establishing distinct protocols for closed-loop task evaluation. We fine-tune the models on simulation datasets tailored to each task. These datasets, derived from the three aforementioned benchmarks, include task instructions and corresponding videos, ensuring the models are well-adapted to the specific embodied scenarios. Finally, the evaluated World Simulator is integrated with the video-to-action model to jointly form an embodied agent that performs the given tasks. The agent’s performance across various tasks serves as a direct measure of the World Simulator’s effectiveness.

Table 3: **The overall performance comparison between Human Preference Evaluator and GPT-4o.** HPE indicates Human Preference Evaluator. HPE@Lavie means that HPE is trained on videos except those generated by Lavie. The validation is conducted on videos generated by Laive under zero-shot setting.

Embodied Scenario	GPT-4o	HPE	GPT-4o@OpenSora	HPE@OpenSora	GPT-4o@Lavie	HPE@Lavie
OE@Acc(↑)	72.8	<b>89.4</b>	66.5	<b>71.6</b>	78.5	<b>87.9</b>
AD@PLCC(↑)	0.28	<b>0.60</b>	0.03	<b>0.34</b>	-0.04	<b>0.49</b>
RM@PLCC(↑)	0.07	<b>0.43</b>	-0.06	<b>0.47</b>	0.17	<b>0.44</b>

**Evaluation Metrics.** In **OE**, we track the MineRL (Guss et al., 2019) environment state to calculate metrics *e.g.*, travel distance and early-game item collection. Travel distance is the agent’s maximum horizontal displacement (X-Z plane) from the spawn point, while dig depth is its maximum vertical displacement (Y axis). We record the maximum number of logs, seeds, and dirt items in the agent’s inventory during the episode. In **AD**, we employ eight widely used evaluation metrics in Carla (Dosovitskiy et al., 2017), including Route Completion (RC), Infraction Score (IS), Driving Score (DS), Vehicle Collisions (VC), Pedestrian Collisions (PC), Layout Collisions (LC), Red Light Violations (RV), and Offroad Infractions (OI). In **RM**, we evaluate the video generation model in the CALVIN (Mees et al., 2022) setting (train on A, B, C → test on D) by running 20 trials and calculating the average success rate.

## 5 EXPERIMENTS

### 5.1 EXPERIMENTAL SETUP

We evaluate 8 popular video generation models, including Open-Sora-Plan(T2V) (Lab & etc., 2024), Lavie (Wang et al., 2023c), ModelScope (Wang et al., 2023b), OpenSora (Zheng et al., 2024), AnimateDiff (Guo et al., 2023), Open-Sora-Plan(TI2V) (Lab & etc., 2024), Dynamicrafter (Xing et al., 2023), EasyAnimate (Xu et al., 2024) through both Explicit Perceptual Evaluation and Implicit Manipulative Evaluation, across three distinct scenarios: **Open-Ended Embodied Environment (OE)**, **Autonomous Driving (AD)**, and **Robot Manipulation (RM)**. All models finetuned on specific datasets corresponding to three embodied scenarios in Explicit Perceptual Evaluation and Implicit Manipulative Evaluation. Detailed information on the datasets, training, and testing configurations can be found in the Supplementary Material.

For Explicit Perceptual Evaluation, we extract five instructions from the Task Instruction Prompt List for each dimension across the three embodied scenarios, ensuring they strongly align with the specific evaluation criteria, as discussed in Sec. 4.1.5. The selected instruction prompts each model to generate five videos, which are then scored by the Human Preference Evaluator to obtain an average score for the model’s performance. For the scoring range 1- $n$ ,  $n$  is set 2 for **OE**, and set 5 for both **AD** and **RM**. We indicate that the generation quality in **OE** is perceived as binary from a human perspective, while the other two scenarios exhibit a more diverse range of video quality.

For Implicit Manipulative Evaluation, we constructed three video-to-action models for embodied simulation environments, following the designs of Steve-1 (Lifshitz et al., 2024), Susie (Black et al., 2023), and LMdrive (Shao et al., 2024). For the evaluated models, we used the following datasets for fine-tuning: (1) VPT (Baker et al., 2022) and our own collected videos along with corresponding task descriptions as the training set for the **OE**; (2) the full Calvin(ABC\_D) (Mees et al., 2022) video dataset and corresponding robot arm control instructions as the training set for **RM**; and (3) the full Carla (Dosovitskiy et al., 2017) video dataset and corresponding autonomous driving navigation commands as the training set for **AD**. Since the video-to-action model in our **OE** setup utilizes a goal-based policy, which interprets the goal from the input video and generates actions based on the current observations and the goal, it allows us to additionally evaluate text-to-video models.

### 5.2 EXPERIMENTS ON HUMAN PREFERENCE EVALUATOR

We demonstrate the strong capabilities and generalization of Human Preference Evaluator by comparing it with GPT-4o (OpenAI, 2024), showcasing its applicability for Explicit Perceptual Evaluation, as shown in Tab. 3. We use accuracy (Acc) in **OE** to assess the alignment of the model with



432  
433  
434  
435  
436  
437  
438  
439  
440  
441  
442  
443  
444  
445  
446  
447  
448  
449  
450  
451  
452  
453  
454  
455  
456  
457  
458  
459  
460  
461  
462  
463  
464  
465  
466  
467  
468  
469  
470  
471  
472  
473  
474  
475  
476  
477  
478  
479  
480  
481  
482  
483  
484  
485

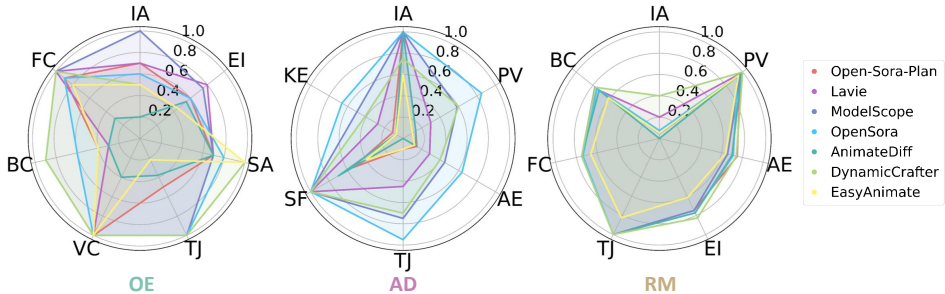


Figure 4: **Result of Explicit Perceptual Evaluation across three embodied scenarios.** Scores in each embodied scenario are normalized to 0-1. The abbreviations are listed in Tab. 2.

human preferences, given the scoring range of 1-2. In contrast, we employ Pearson linear correlation coefficient (PLCC) for **AD** and **RM** as their scores range from 1-5.

After fine-tuning on HF-Embodied Dataset, our evaluator consistently surpasses the performance of GPT-4o in terms of alignment with human preferences across all scenarios. Additionally, we conducted zero-shot experiments with two challenging models, *i.e.* OpenSora and Lavie. GPT-4o exhibits a negative correlation with human preferences in evaluating OpenSora in **AD** under zero-shot setting, as well as evaluating Lavie in **RM** under zero-shot setting. Our evaluator’s zero-shot performance shows a high correlation with human preferences, further demonstrating its robust generalization capabilities. Human Preference Evaluator is suitable for Explicit Perceptual Evaluation, and the HF-Embodied Dataset can be leveraged to train even more aligned models for assessing video generation models towards World Simulators. More details in Sup. B.3.

### 5.3 DESIGN FEATURES AND DISCUSSIONS

In this section, we discuss the Design features and corresponding observations we draw from our comprehensive evaluation experiments. More details can be found in the Supplementary Material.

**Human Preference with Feedback.** Given the complexity and diversity in the representation of physical rules in videos, even a specific dimension may manifest in various ways (for example, both illogical and discontinuous object motion fall under trajectory-related issues). This makes it challenging to evaluate using score-based models or a single fixed set of evaluation criteria. WorldSim-Bench addresses this challenge effectively by employing a human preference scoring mechanism and a fine-grained feedback system. Fig. 4 illustrates the evaluation results of Explicit Perceptual Evaluation, more detail analyze could be found in Sup. C. In **OE**, most models struggle with Embodied Interaction, particularly in generating plausible object deformations, *e.g.*, block shattering, due to the complexity of physical rules. In **AD**, the variation between models is minimal, with high-performing models excelling across all dimensions. The simpler instructions, like moving forward or turning, lead to high Instruction Alignment, but many generated videos suffer from poor 3D depth (Perspectivity) and fail to depict realistic embodied elements like pedestrians and vehicles, affecting the overall Aesthetic. In **RM**, models perform uniformly well in static scene depiction, excelling in Perspectivity and Foreground/Background Consistency. However, they struggle with Instruction Alignment, often generating aimless actions. Despite this, the lack of unreasonable trajectories results in relatively high Trajectory scores, though robotic manipulation remains a significant challenge for current models.

**Close-loop Interactive Evaluation.** Given the dynamic nature and real-time requirements of interactive environments, evaluating World Simulators through static benchmarks often fails to capture the full spectrum of their capabilities. Close-loop Interactive Evaluation addresses this by enabling continuous feedback and adaptation, ensuring that the model’s predictions and actions evolve in response to the changing environment, thus providing a more accurate and realistic assessment of its performance. Fig. 5 presents the Implicit Manipulative Evaluation results, showing significant variation in the performance of video generation models across different tasks. In the **OE**, video generation models conditioned on the first frame have a significantly lower success rate compared to those without image conditioning. This suggests that models with image conditioning struggle to generate physical laws and 3D scene representations accurately. Tasks like travel, requiring high-quality trajectories and 3D representation, show the greatest variation in model performance, while

486  
487  
488  
489  
490  
491  
492  
493  
494  
495  
496  
497  
498  
499  
500  
501  
502  
503  
504  
505  
506  
507  
508  
509  
510  
511  
512  
513  
514  
515  
516  
517  
518  
519  
520  
521  
522  
523  
524  
525  
526  
527  
528  
529  
530  
531  
532  
533  
534  
535  
536  
537  
538  
539

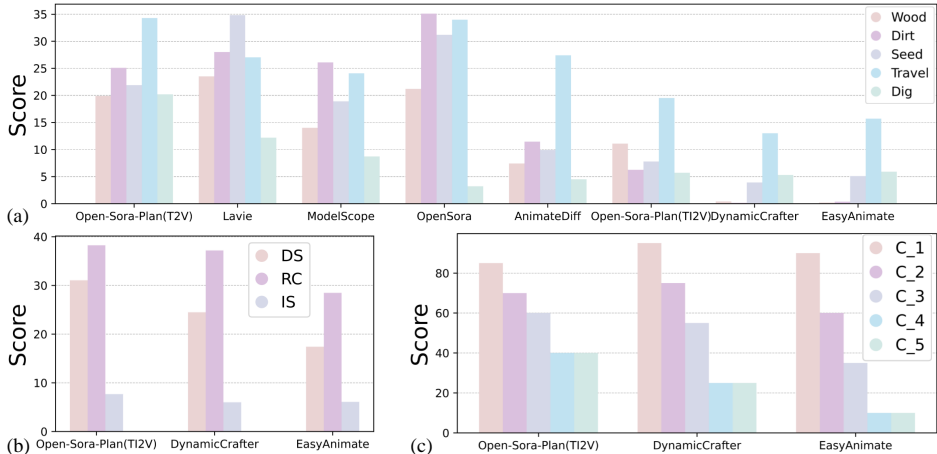


Figure 5: **Result of Implicit Manipulative Evaluation across three embodied scenarios.**The abbreviations are listed in Sec. 4.2.2.

simpler tasks like collecting wood see similar performance across models, indicating effective handling of minimal background variation. In the AD, models with better trajectory(Open-Sora-Plan) generation perform better. In the RM, where background variation is minimal, models perform similarly on simple tasks, but as complexity increases, more robust models achieve higher success rates. Despite some success across scenarios, video generation models still need significant improvements in generating physically consistent content to be reliable for training agents or guiding actions.

**Alignment of Physical Rules and Actions.** Ensuring that World Simulators adhere to physical laws while generating predictions is crucial for practical application. The alignment of physical rules and actions is essential as it guarantees that the model’s outputs are not only visually plausible but also executable in real-world scenarios. This approach allows for the seamless integration of predicted actions with their physical environment, ensuring reliability and effectiveness in real-world tasks. Based on our experimental findings, we observe that most conclusions from the Explicit Perceptual Evaluation and Implicit Manipulative Evaluation evaluations are consistent. Specifically, the visual quality across most dimensions aligns with the results from the closed-loop experiments. *e.g.*, Dynamicrafter, which performs well in trajectory generation in Explicit Perceptual Evaluation, also excels in trajectory-focused scenarios like AD and RM. However, in other cases—such as the OE, which requires more frequent interactions, and long-sequence tasks (4, 5) in RM—Dynamicrafter underperforms compared to Open-Sora-Plan. This differs from the Explicit Perceptual Evaluation results, likely because these tasks demand stable, high-quality video generation for guidance, where Open-Sora-Plan shows higher robustness. Therefore, a comprehensive evaluation of video generation models requires a combination of Explicit Perceptual Evaluation and Implicit Manipulative Evaluation assessments to provide the most fair and accurate judgment. Finally, based on the overall Explicit Perceptual Evaluation and Implicit Manipulative Evaluation results, we conclude that current video generation models still fail to effectively capture many physical rules, indicating significant improvements are needed before they can function as true World Simulators.

## 6 CONCLUSION

In this work, we classify the functionalities of predictive models into a hierarchy and take the first step in evaluating World Simulators by proposing a dual evaluation framework called WorldSim-Bench. We conducted a comprehensive evaluation and analysis of multiple video generation models as World Simulators through both Explicit Perceptual Evaluation and Implicit Manipulative Evaluation processes. We summarize key findings from the evaluation and hope these insights will inspire and guide future research on World Simulators.

**Limitations.** Although we evaluate physical rules and 3D content from the perspective of embodied intelligence, the World Simulator can be applied to more scenarios than just robots, and different scenarios have more physical representations, so how to effectively evaluate the World Simulator in other scenarios requires more exploration.

## REFERENCES

- 540  
541  
542 Josh Achiam, Steven Adler, Sandhini Agarwal, Lama Ahmad, Ilge Akkaya, Florencia Leoni Ale-  
543 man, Diogo Almeida, Janko Altenschmidt, Sam Altman, Shyamal Anadkat, et al. Gpt-4 technical  
544 report. *arXiv preprint arXiv:2303.08774*, 2023.
- 545 Max Bain, Arsha Nagrani, Gül Varol, and Andrew Zisserman. Frozen in time: A joint video and  
546 image encoder for end-to-end retrieval. In *Proceedings of the IEEE/CVF international conference*  
547 *on computer vision*, pp. 1728–1738, 2021.
- 548 Bowen Baker, Ilge Akkaya, Peter Zhokov, Joost Huizinga, Jie Tang, Adrien Ecoffet, Brandon  
549 Houghton, Raul Sampedro, and Jeff Clune. Video pretraining (vpt): Learning to act by watching  
550 unlabeled online videos. *Advances in Neural Information Processing Systems*, 35:24639–24654,  
551 2022.
- 552 Kevin Black, Mitsuhiro Nakamoto, Pranav Atreya, Homer Walke, Chelsea Finn, Aviral Kumar, and  
553 Sergey Levine. Zero-shot robotic manipulation with pretrained image-editing diffusion models.  
554 *arXiv preprint arXiv:2310.10639*, 2023.
- 555 Tim Brooks, Aleksander Holynski, and Alexei A Efros. Instructpix2pix: Learning to follow image  
556 editing instructions. In *Proceedings of the IEEE/CVF Conference on Computer Vision and Pattern*  
557 *Recognition*, pp. 18392–18402, 2023.
- 558 Holger Caesar, Varun Bankiti, Alex H Lang, Sourabh Vora, Venice Erin Liong, Qiang Xu, Anush  
559 Krishnan, Yu Pan, Giancarlo Baldan, and Oscar Beijbom. nuscenes: A multimodal dataset for  
560 autonomous driving. In *Proceedings of the IEEE/CVF conference on computer vision and pattern*  
561 *recognition*, pp. 11621–11631, 2020.
- 562 Yi Chen, Yuying Ge, Yixiao Ge, Mingyu Ding, Bohao Li, Rui Wang, Ruifeng Xu, Ying Shan, and  
563 Xihui Liu. Egoplan-bench: Benchmarking egocentric embodied planning with multimodal large  
564 language models. *arXiv preprint arXiv:2312.06722*, 2023.
- 565 Zeren Chen, Zhelun Shi, Xiaoya Lu, Lehan He, Sucheng Qian, Hao Shu Fang, Zhenfei Yin, Wanli  
566 Ouyang, Jing Shao, Yu Qiao, et al. Rh20t-p: A primitive-level robotic dataset towards composable  
567 generalization agents. *arXiv preprint arXiv:2403.19622*, 2024.
- 568 Wei-Lin Chiang, Zhuohan Li, Zi Lin, Ying Sheng, Zhanghao Wu, Hao Zhang, Lianmin Zheng,  
569 Siyuan Zhuang, Yonghao Zhuang, Joseph E Gonzalez, et al. Vicuna: An open-source chatbot  
570 impressing gpt-4 with 90%\* chatgpt quality. See <https://vicuna.lmsys.org> (accessed 14 April  
571 2023), 2023.
- 572 Alexey Dosovitskiy, German Ros, Felipe Codevilla, Antonio Lopez, and Vladlen Koltun. Carla: An  
573 open urban driving simulator. In *Conference on robot learning*, pp. 1–16. PMLR, 2017.
- 574 Danny Driess, Fei Xia, Mehdi SM Sajjadi, Corey Lynch, Aakanksha Chowdhery, Brian Ichter,  
575 Ayzaan Wahid, Jonathan Tompson, Quan Vuong, Tianhe Yu, et al. Palm-e: An embodied multi-  
576 modal language model. *arXiv preprint arXiv:2303.03378*, 2023.
- 577 Yilun Du, Mengjiao Yang, Pete Florence, Fei Xia, Ayzaan Wahid, Brian Ichter, Pierre Sermanet,  
578 Tianhe Yu, Pieter Abbeel, Joshua B Tenenbaum, et al. Video language planning. *arXiv preprint*  
579 *arXiv:2310.10625*, 2023.
- 580 Yilun Du, Sherry Yang, Bo Dai, Hanjun Dai, Ofir Nachum, Josh Tenenbaum, Dale Schuurmans, and  
581 Pieter Abbeel. Learning universal policies via text-guided video generation. *Advances in Neural*  
582 *Information Processing Systems*, 36, 2024.
- 583 Frederik Ebert, Yanlai Yang, Karl Schmeckpeper, Bernadette Bucher, Georgios Georgakis, Kostas  
584 Daniilidis, Chelsea Finn, and Sergey Levine. Bridge data: Boosting generalization of robotic  
585 skills with cross-domain datasets. *arXiv preprint arXiv:2109.13396*, 2021.
- 586 Hao-Shu Fang, Hongjie Fang, Zhenyu Tang, Jirong Liu, Junbo Wang, Haoyi Zhu, and Cewu Lu.  
587 Rh20t: A robotic dataset for learning diverse skills in one-shot. In *RSS 2023 Workshop on Learn-*  
588 *ing for Task and Motion Planning*, 2023.

- 594 Tsu-Jui Fu, Wenze Hu, Xianzhi Du, William Yang Wang, Yinfei Yang, and Zhe Gan. Guid-  
595 ing instruction-based image editing via multimodal large language models. *arXiv preprint*  
596 *arXiv:2309.17102*, 2023.
- 597
- 598 Shenyuan Gao, Jiazhi Yang, Li Chen, Kashyap Chitta, Yihang Qiu, Andreas Geiger, Jun Zhang,  
599 and Hongyang Li. Vista: A generalizable driving world model with high fidelity and versatile  
600 controllability. *arXiv preprint arXiv:2405.17398*, 2024.
- 601
- 602 Raghav Goyal, Samira Ebrahimi Kahou, Vincent Michalski, Joanna Materzynska, Susanne West-  
603 phal, Heuna Kim, Valentin Haenel, Ingo Fruend, Peter Yianilos, Moritz Mueller-Freitag, et al.  
604 The” something something” video database for learning and evaluating visual common sense. In  
605 *Proceedings of the IEEE international conference on computer vision*, pp. 5842–5850, 2017.
- 606
- 607 Kristen Grauman, Andrew Westbury, Eugene Byrne, Zachary Chavis, Antonino Furnari, Rohit Gird-  
608 har, Jackson Hamburger, Hao Jiang, Miao Liu, Xingyu Liu, et al. Ego4d: Around the world in  
609 3,000 hours of egocentric video. In *Proceedings of the IEEE/CVF Conference on Computer Vision*  
*and Pattern Recognition*, pp. 18995–19012, 2022.
- 610
- 611 Yuwei Guo, Ceyuan Yang, Anyi Rao, Zhengyang Liang, Yaohui Wang, Yu Qiao, Maneesh  
612 Agrawala, Dahua Lin, and Bo Dai. Animatediff: Animate your personalized text-to-image diffu-  
613 sion models without specific tuning. *arXiv preprint arXiv:2307.04725*, 2023.
- 614
- 615 William H Guss, Brandon Houghton, Nicholay Topin, Phillip Wang, Cayden Codel, Manuela  
616 Veloso, and Ruslan Salakhutdinov. Minerl: A large-scale dataset of minecraft demonstrations.  
*arXiv preprint arXiv:1907.13440*, 2019.
- 617
- 618 David Ha and Jürgen Schmidhuber. World models. *arXiv preprint arXiv:1803.10122*, 2018.
- 619
- 620 Xuehai He, Weixi Feng, Kaizhi Zheng, Yujie Lu, Wanrong Zhu, Jiachen Li, Yue Fan, Jianfeng Wang,  
621 Linjie Li, Zhengyuan Yang, et al. Mmworld: Towards multi-discipline multi-faceted world model  
622 evaluation in videos. *arXiv preprint arXiv:2406.08407*, 2024.
- 623
- 624 Edward J. Hu, Yelong Shen, Phillip Wallis, Zeyuan Allen-Zhu, Yuanzhi Li, Shean Wang, Lu Wang,  
and Weizhu Chen. Lora: Low-rank adaptation of large language models, 2021.
- 625
- 626 Ziqi Huang, Yinan He, Jiashuo Yu, Fan Zhang, Chenyang Si, Yuming Jiang, Yuanhan Zhang, Tianx-  
627 ing Wu, Qingyang Jin, Nattapol Chanpaisit, et al. Vbench: Comprehensive benchmark suite for  
628 video generative models. In *Proceedings of the IEEE/CVF Conference on Computer Vision and*  
*Pattern Recognition*, pp. 21807–21818, 2024.
- 629
- 630 Michael Janner, Yilun Du, Joshua B Tenenbaum, and Sergey Levine. Planning with diffusion for  
631 flexible behavior synthesis. *arXiv preprint arXiv:2205.09991*, 2022.
- 632
- 633 PKU-Yuan Lab and Tuzhan AI etc. Open-sora-plan, April 2024. URL [https://doi.org/10.](https://doi.org/10.5281/zenodo.10948109)  
634 [5281/zenodo.10948109](https://doi.org/10.5281/zenodo.10948109).
- 635
- 636 Bolin Lai, Xiaoliang Dai, Lawrence Chen, Guan Pang, James M Rehg, and Miao Liu. Lego:  
637 Learning egocentric action frame generation via visual instruction tuning. *arXiv preprint*  
*arXiv:2312.03849*, 2023.
- 638
- 639 Xiaoqi Li, Mingxu Zhang, Yiran Geng, Haoran Geng, Yuxing Long, Yan Shen, Renrui Zhang,  
640 Jiaming Liu, and Hao Dong. Manipllm: Embodied multimodal large language model for object-  
641 centric robotic manipulation. In *Proceedings of the IEEE/CVF Conference on Computer Vision*  
*and Pattern Recognition*, pp. 18061–18070, 2024.
- 642
- 643 Shalev Lifshitz, Keiran Paster, Harris Chan, Jimmy Ba, and Sheila McIlraith. Steve-1: A generative  
644 model for text-to-behavior in minecraft. *Advances in Neural Information Processing Systems*, 36,  
645 2024.
- 646
- 647 Haotian Liu, Chunyuan Li, Qingyang Wu, and Yong Jae Lee. Visual instruction tuning. In *NeurIPS*,  
2023a.

- 648 Xiao Liu, Hao Yu, Hanchen Zhang, Yifan Xu, Xuanyu Lei, Hanyu Lai, Yu Gu, Hangliang Ding,  
649 Kaiwen Men, Kejuan Yang, et al. Agentbench: Evaluating llms as agents. *arXiv preprint*  
650 *arXiv:2308.03688*, 2023b.
- 651 Xiao Liu, Tianjie Zhang, Yu Gu, Iat Long Iong, Yifan Xu, Xixuan Song, Shudan Zhang, Hanyu Lai,  
652 Xinyi Liu, Hanlin Zhao, et al. Visualagentbench: Towards large multimodal models as visual  
653 foundation agents. *arXiv preprint arXiv:2408.06327*, 2024a.
- 654 Yaofang Liu, Xiaodong Cun, Xuebo Liu, Xintao Wang, Yong Zhang, Haoxin Chen, Yang Liu,  
655 Tiejong Zeng, Raymond Chan, and Ying Shan. Evalcrafter: Benchmarking and evaluating large  
656 video generation models. In *Proceedings of the IEEE/CVF Conference on Computer Vision and*  
657 *Pattern Recognition*, pp. 22139–22149, 2024b.
- 658 Chaochao Lu, Chen Qian, Guodong Zheng, Hongxing Fan, Hongzhi Gao, Jie Zhang, Jing Shao,  
659 Jingyi Deng, Jinlan Fu, Kexin Huang, Kunchang Li, Lijun Li, Limin Wang, Lu Sheng, Meiqi  
660 Chen, Ming Zhang, Qibing Ren, Sirui Chen, Tao Gui, Wanli Ouyang, Yali Wang, Yan Teng, Yaru  
661 Wang, Yi Wang, Yinan He, Yingchun Wang, Yixu Wang, Yongting Zhang, Yu Qiao, Yujiong  
662 Shen, Yurong Mou, Yuxi Chen, Zaibin Zhang, Zhelun Shi, Zhenfei Yin, and Zhipin Wang. From  
663 gpt-4 to gemini and beyond: Assessing the landscape of mllms on generalizability, trustworthiness  
664 and causality through four modalities, 2024.
- 665 Oier Mees, Lukas Hermann, Erick Rosete-Beas, and Wolfram Burgard. Calvin: A benchmark for  
666 language-conditioned policy learning for long-horizon robot manipulation tasks. *IEEE Robotics*  
667 *and Automation Letters*, 7(3):7327–7334, 2022.
- 668 OpenAI. Gpt-4o. <https://openai.com/index/hello-gpt-4o/>, 2024.
- 669 William Peebles and Saining Xie. Scalable diffusion models with transformers. In *Proceedings of*  
670 *the IEEE/CVF International Conference on Computer Vision*, pp. 4195–4205, 2023.
- 671 Yiran Qin, Enshen Zhou, Qichang Liu, Zhenfei Yin, Lu Sheng, Ruimao Zhang, Yu Qiao, and Jing  
672 Shao. Mp5: A multi-modal open-ended embodied system in minecraft via active perception. In  
673 *2024 IEEE/CVF Conference on Computer Vision and Pattern Recognition (CVPR)*, pp. 16307–  
674 16316. IEEE, 2024.
- 675 Alec Radford, Jeffrey Wu, Rewon Child, David Luan, Dario Amodei, Ilya Sutskever, et al. Language  
676 models are unsupervised multitask learners. *OpenAI blog*, 1(8):9, 2019.
- 677 Hao Shao, Yuxuan Hu, Letian Wang, Guanglu Song, Steven L Waslander, Yu Liu, and Hongsheng  
678 Li. Lmdrive: Closed-loop end-to-end driving with large language models. In *Proceedings of the*  
679 *IEEE/CVF Conference on Computer Vision and Pattern Recognition*, pp. 15120–15130, 2024.
- 680 Zhelun Shi, Zhipin Wang, Hongxing Fan, Zaibin Zhang, Lijun Li, Yongting Zhang, Zhenfei Yin,  
681 Lu Sheng, Yu Qiao, and Jing Shao. Assessment of multimodal large language models in alignment  
682 with human values, 2024.
- 683 Gemini Team, Rohan Anil, Sebastian Borgeaud, Yonghui Wu, Jean-Baptiste Alayrac, Jiahui Yu,  
684 Radu Soricut, Johan Schalkwyk, Andrew M Dai, Anja Hauth, et al. Gemini: a family of highly  
685 capable multimodal models. *arXiv preprint arXiv:2312.11805*, 2023.
- 686 Hugo Touvron, Thibaut Lavril, Gautier Izacard, Xavier Martinet, Marie-Anne Lachaux, Timothée  
687 Lacroix, Baptiste Rozière, Naman Goyal, Eric Hambro, Faisal Azhar, et al. Llama: Open and  
688 efficient foundation language models. *arXiv preprint arXiv:2302.13971*, 2023.
- 689 Guanzhi Wang, Yuqi Xie, Yunfan Jiang, Ajay Mandlekar, Chaowei Xiao, Yuke Zhu, Linxi Fan,  
690 and Anima Anandkumar. Voyager: An open-ended embodied agent with large language models.  
691 *arXiv preprint arXiv:2305.16291*, 2023a.
- 692 Jiuniu Wang, Hangjie Yuan, Dayou Chen, Yingya Zhang, Xiang Wang, and Shiwei Zhang. Mod-  
693 elscape text-to-video technical report. *arXiv preprint arXiv:2308.06571*, 2023b.
- 694 Yaohui Wang, Xinyuan Chen, Xin Ma, Shangchen Zhou, Ziqi Huang, Yi Wang, Ceyuan Yang, Yinan  
695 He, Jiashuo Yu, Peiqing Yang, et al. Lavie: High-quality video generation with cascaded latent  
696 diffusion models. *arXiv preprint arXiv:2309.15103*, 2023c.



702 Zihao Wang, Shaofei Cai, Guanzhou Chen, Anji Liu, Xiaojian Ma, and Yitao Liang. Describe,  
703 explain, plan and select: Interactive planning with large language models enables open-world  
704 multi-task agents. *arXiv preprint arXiv:2302.01560*, 2023d.

705  
706 Jinbo Xing, Menghan Xia, Yong Zhang, Haoxin Chen, Xintao Wang, Tien-Tsin Wong, and Ying  
707 Shan. Dynamicrafter: Animating open-domain images with video diffusion priors. *arXiv preprint*  
708 *arXiv:2310.12190*, 2023.

709 Jiaqi Xu, Xinyi Zou, Kunzhe Huang, Yunkuo Chen, Bo Liu, MengLi Cheng, Xing Shi, and Jun  
710 Huang. Easyanimate: A high-performance long video generation method based on transformer  
711 architecture. *arXiv preprint arXiv:2405.18991*, 2024.

712  
713 Mengjiao Yang, Yilun Du, Kamyar Ghasemipour, Jonathan Tompson, Dale Schuurmans, and Pieter  
714 Abbeel. Learning interactive real-world simulators. *arXiv preprint arXiv:2310.06114*, 2023.

715 Zhenfei Yin, Jiong Wang, Jianjian Cao, Zhelun Shi, Dingning Liu, Mukai Li, Xiaoshui Huang,  
716 Zhiyong Wang, Lu Sheng, Lei Bai, Jing Shao, and Wanli Ouyang. LAMM: language-assisted  
717 multi-modal instruction-tuning dataset, framework, and benchmark. In *NeurIPS*, 2023.

718  
719 Sihyun Yu, Kihyuk Sohn, Subin Kim, and Jinwoo Shin. Video probabilistic diffusion models in  
720 projected latent space. In *Proceedings of the IEEE/CVF conference on computer vision and*  
721 *pattern recognition*, pp. 18456–18466, 2023.

722 Haoji Zhang, Yiqin Wang, Yansong Tang, Yong Liu, Jiashi Feng, Jifeng Dai, and Xiaojie Jin. Flash-  
723 vstream: Memory-based real-time understanding for long video streams, 2024a.

724  
725 Zaibin Zhang, Shiyu Tang, Yuanhang Zhang, Talas Fu, Yifan Wang, Yang Liu, Dong Wang, Jing  
726 Shao, Lijun Wang, and Huchuan Lu. Ad-h: Autonomous driving with hierarchical agents. *arXiv*  
727 *preprint arXiv:2406.03474*, 2024b.

728 Zangwei Zheng, Xiangyu Peng, Tianji Yang, Chenhui Shen, Shenggui Li, Hongxin Liu, Yukun  
729 Zhou, Tianyi Li, and Yang You. Open-sora: Democratizing efficient video production for all,  
730 March 2024. URL <https://github.com/hpcaitech/Open-Sora>.

731  
732 Enshen Zhou, Yiran Qin, Zhenfei Yin, Yuzhou Huang, Ruimao Zhang, Lu Sheng, Yu Qiao, and  
733 Jing Shao. Minedreamer: Learning to follow instructions via chain-of-imagination for simulated-  
734 world control. *arXiv preprint arXiv:2403.12037*, 2024.

735  
736  
737  
738  
739  
740  
741  
742  
743  
744  
745  
746  
747  
748  
749  
750  
751  
752  
753  
754  
755

## Part I

## Appendix

## Table of Contents

---

<b>A</b>	<b>Taxonomy in Explicit Perceptual Evaluation</b>	<b>16</b>
A.1	Open-Ended Embodied Environment . . . . .	16
A.2	Autonomous Driving . . . . .	16
A.3	Robot Manipulation . . . . .	16
<b>B</b>	<b>Detailed Implementation of Explicit Perceptual Evaluation</b>	<b>17</b>
B.1	HF-Embodied Dataset . . . . .	17
B.2	Video Generation Model Finetuning . . . . .	17
B.3	Human Preference Evaluator Training . . . . .	18
<b>C</b>	<b>Detailed Result of Explicit Perceptual Evaluation</b>	<b>19</b>
C.1	Quantitative Results . . . . .	19
C.2	Qualitative Results . . . . .	21
<b>D</b>	<b>Implicit Manipulative Evaluation-OE</b>	<b>21</b>
D.1	Detailed Description . . . . .	21
D.2	Actions . . . . .	22
D.3	Full Result . . . . .	22
D.4	Roll Out . . . . .	23
<b>E</b>	<b>Implicit Manipulative Evaluation-AD</b>	<b>23</b>
E.1	Detailed Description . . . . .	24
E.2	Actions . . . . .	24
E.3	Full Result . . . . .	25
E.4	Roll Out . . . . .	25
<b>F</b>	<b>Implicit Manipulative Evaluation-RM</b>	<b>25</b>
F.1	Detailed Description . . . . .	25
F.2	Actions . . . . .	26
F.3	Full Result . . . . .	26
F.4	Roll Out . . . . .	27
<b>G</b>	<b>Discussion of Vision-Language-Action Models</b>	<b>27</b>

---

## 810 A TAXONOMY IN EXPLICIT PERCEPTUAL EVALUATION

811  
812  
813 We outline the evaluation dimensions for each embodied scenario below, along with their corre-  
814 sponding explanations. These explanations are used for detailed human annotation documentation  
815 and also serve as the explanation of the evaluation criteria in instructions for the Human Preference  
816 Evaluator.

### 817 818 819 A.1 OPEN-ENDED EMBODIED ENVIRONMENT

820  
821 **Visual Quality.** Background Consistency ensures the background remains consistent throughout  
822 the video. Foreground Consistency verifies the consistency of the foreground elements.

823 **Condition Consistency.** Instruction Alignment assesses whether the video aligns with the provided  
824 input instruction. Scenario Alignment checks if the input instruction defines an embodied scenario  
825 and whether the video accurately reflects this scenario.

826 **Embodiment.** Velocity evaluates if the velocity of the observed object is appropriate. Embodied  
827 Interaction evaluates the embodied interaction’s appropriateness based on the interaction process  
828 and target. Trajectory evaluates whether the motion trajectory in the video is logical.

### 829 830 831 A.2 AUTONOMOUS DRIVING

832  
833 **Visual Quality.** Aesthetics evaluates whether the composition, color, lighting, and scene in the  
834 video align with human aesthetics.

835  
836 **Condition Consistency.** Instruction Alignment assesses whether the video aligns with the provided  
837 input instruction.

838 **Embodiment.** Perspectivity evaluates the video’s perspective, specifically assessing the 3D scene  
839 relationships. This includes evaluating whether the video has a strong sense of depth and realism  
840 (*i.e.*, whether it feels three-dimensional). Additionally, assess the logic of lighting and shadows,  
841 including whether the shadow positions are consistent with the light sources. Trajectory evaluates  
842 whether the movement and the trajectory of elements in the video is logical. Key Element assesses  
843 the generated quality of embodied elements *e.g.*, roads, vehicles, pedestrians, bicycles, lane mark-  
844 ings, sidewalks, traffic signs, and traffic lights. Safety evaluates whether the behavior of the vehicles  
845 comply with traffic rules. Are there any instances of running red lights, speeding, or driving outside  
846 of permissible areas.

### 847 848 849 A.3 ROBOT MANIPULATION

850  
851 **Visual Quality.** Aesthetics evaluates whether the composition, color, lighting, and scene in the video  
852 align with human aesthetics. Background Consistency ensures the background remains consistent  
853 throughout the video, include the manipulation table and the environment. Foreground Consistency  
854 verifies the consistency of the foreground elements, including the robotic arm and the object on the  
855 manipulation table.

856 **Condition Consistency.** Instruction Alignment assesses whether the action of the robot arm in the  
857 generated video aligns with the provided input instruction.

858 **Embodiment.** Perspectivity evaluates the video’s perspective, specifically assessing the 3D scene  
859 relationships. This includes evaluating whether the video has a strong sense of depth and realism  
860 (*i.e.*, whether it feels three-dimensional). Additionally, assess the logic of lighting and shadows,  
861 including whether the shadow positions are consistent with the light sources. Embodied Interaction  
862 judges whether the object’s shape and posture conform to the rules during the collision of objects and  
863 the interaction between the robotic arm and the object. Trajectory evaluates whether the trajectory  
of the robotic arm is reasonable and in line with human cognition.

Table 4: **Analysis of HF-Embodied Dataset.** Samples scored higher than 3 in **AD** and **RM** are considered positive.

Embodied Scenario	#instructions	#videos	#dims	#actions	#positive	#negative
Open-Ended Embodied Environment	270	8401	7	11	121249	79965
Autonomous Driving	5	15870	6	5	56768	35044
Robot Manipulation	2556	11430	7	26	70672	9338

## B DETAILED IMPLEMENTATION OF EXPLICIT PERCEPTUAL EVALUATION

### B.1 HF-EMBODIED DATASET

Tab. 4 provides an analysis of the HF-Embodied Dataset. In **Autonomous Driving** scenario, there are only five instructions: move forward, move backward, turn left, turn right, and stop. The other two scenarios include a variety of instructions that combine actions with target objects. Given the diverse instructions, different video generation models generate multiple videos after finetuning on specific datasets. To enhance the Human Preference Evaluator understanding of the autonomous driving context, we also supplement the **AD** scenario with videos from real-world scenes. Additionally, we list the quantities of positive and negative samples across all dimensions. Samples with human annotated scores of 3 or higher in **AD** and **RM** are considered positive. Leveraging HF-Embodied Dataset with comprehensive embodied dimensions, we train the Human Preference Evaluator to enable efficient assessment in Explicit Perceptual Evaluation.

**Discussion of Future Work.** Human Preference Evaluator (HPE) and HF-Embodied Dataset have been effective in aligning generated content with human preferences and evaluating video generation models, and we could explore more about its potential applications. Here are some future work directions to leverage the capabilities of HPE and HF-Embodied Dataset:

**Interactive Training for Generative Models** Utilize HPE as a real-time feedback mechanism during the training of generative models. By integrating HPE and HF-Embodied Dataset into a reinforcement learning framework, it could dynamically guide the model to improve alignment with human preferences across various scenarios, and can even make the world simulator perform better in downstream tasks.

### B.2 VIDEO GENERATION MODEL FINETUNING

Table 5: **Training Frames of Generation Models.**

Model	Open-Sora-Plan	Lavie	ModelScope	OpenSora	AnimateDiff	DynamicCrafter	EasyAnimate
Short Videos(frames)	16	16	16	16	16	16	16
Long Videos(frames)	64	48	60	48	64	60	64

We evaluate 8 popular video generation model, including Open-Sora-Plan(T2V) (Lab & etc., 2024), Lavie (Wang et al., 2023c), ModelScope (Wang et al., 2023b), OpenSora (Zheng et al., 2024), AnimateDiff (Guo et al., 2023), Open-Sora-Plan(TI2V) (Lab & etc., 2024), DynamicCrafter (Xing et al., 2023), EasyAnimate (Xu et al., 2024) through both Explicit Perceptual Evaluation and Implicit Manipulative Evaluation, across three distinct scenarios: **Open-Ended Embodied Environment (OE)**, **Autonomous Driving (AD)**, and **Robot Manipulation (RM)**.

In **Open-Ended Embodied Environment**, we use **OpenAI Contractor Gameplay Dataset** (Baker et al., 2022) which is created by hiring human contractors to play Minecraft and complete tasks like house building. Keypresses and mouse movements are recorded during gameplay. We apply the same preprocessing steps as VPT, including filtering out null actions. Additionally, we create a supplementary dataset for the task "Explore" by generating trajectories using various pre-trained Steve-1 agents. The distribution of this dataset is enhanced by randomly switching between models during trajectories, resetting the agent’s memory, and adjusting the agent’s orientation to face new directions at random intervals. For specific in-game events, e.g., "mine\_block", the type of block broken is logged alongside precise timestamps. These timestamps allow for accurate progress tracking and are aligned with the completion of event-related instructions.

918	OE@Acc(↑)	BC	FC	IA	SA	VC	TJ	EI	Overall
919	GPT-4o	60.5	70.4	70.9	67.3	79.6	83.7	85.9	72.8
920	HPE	<b>81.2</b>	<b>87.5</b>	<b>87.5</b>	<b>96.4</b>	<b>94.5</b>	<b>93.8</b>	<b>88.8</b>	<b>89.4</b>
921	GPT-4o@OpenSora	60	80	<b>80</b>	50	0.0	<b>100</b>	<b>88.8</b>	66.5
922	HPE@OpenSora	<b>70</b>	<b>90</b>	60	<b>100</b>	<b>100</b>	22.2	80	<b>71.6</b>
923	GPT-4o@Lavie	50	66.7	75	88.8	<b>87.5</b>	<b>100</b>	87.5	78.5
924	HPE@Lavie	<b>80</b>	<b>80</b>	<b>80</b>	<b>100</b>	<b>100</b>	75	<b>100</b>	<b>87.9</b>
925	AD@PLCC(↑)	AE	IA	PV	TJ	KE	SF	Overall	
926	GPT-4o	0.37	0.22	0.23	0.28	0.37	0.18	0.28	
927	HPE	<b>0.71</b>	<b>0.57</b>	<b>0.50</b>	<b>0.58</b>	<b>0.65</b>	<b>0.58</b>	<b>0.60</b>	
928	GPT-4o@OpenSora	0.22	-0.39	0.32	<b>0.15</b>	-0.03	-0.12	0.03	
929	HPE@OpenSora	<b>0.37</b>	<b>0.55</b>	<b>0.34</b>	0.06	<b>0.28</b>	<b>0.41</b>	<b>0.34</b>	
930	GPT-4o@Lavie	0.17	0.13	-0.34	0.06	-0.09	-0.15	-0.04	
931	HPE@Lavie	<b>0.28</b>	<b>1.0</b>	<b>0.49</b>	<b>0.37</b>	<b>0.12</b>	<b>0.69</b>	<b>0.49</b>	
932	RM@PLCC(↑)	AE	BC	FC	IA	PV	TJ	EI	Overall
933	GPT-4o	0.07	0.18	0.20	0.32	-0.14	-0.01	-0.14	0.07
934	HPE	<b>0.52</b>	<b>0.43</b>	<b>0.43</b>	<b>0.43</b>	<b>0.20</b>	<b>0.56</b>	<b>0.44</b>	<b>0.43</b>
935	GPT-4o@OpenSora	-0.45	-0.03	<b>0.08</b>	0.0	0.04	-0.23	0.14	-0.06
936	HPE@OpenSora	<b>0.25</b>	<b>0.35</b>	0.05	<b>0.42</b>	<b>0.89</b>	<b>0.89</b>	<b>0.44</b>	<b>0.47</b>
937	GPT-4o@Lavie	0.11	-0.07	0.42	<b>0.42</b>	0.21	0.31	-0.21	0.17
938	HPE@Lavie	<b>0.33</b>	<b>0.04</b>	<b>0.69</b>	0.40	<b>0.89</b>	<b>0.67</b>	<b>0.06</b>	<b>0.44</b>
939									
940									
941									

Table 6: **Performance comparison between Human Preference Evaluator and GPT-4o.** HPE indicates Human Preference Evaluator. The other abbreviations are listed in Tab. 2.

In **Autonomous Driving**, we fine-tune using the nuScenes training set (Caesar et al., 2020), and following the approach in Vista (Gao et al., 2024), we sample video clips consisting of 25 frames at a frequency of 10 Hz. To classify actions into textual commands, we adhere to established conventions in planning and define ego-vehicle commands as “turn right”, “turn left”, “go straight”, and “stop”, consistent with the definitions in Vista.

In **Robot Manipulation**, we use RH20T-P (Chen et al., 2024), a dataset based on RH20T (Fang et al., 2023) and designed for primitive-level robotic manipulation that features meticulously defined primitive skills and diverse primitive-level spatial knowledge of multiple forms. We use each primitive-level robotic manipulation instruction along with the corresponding video as input for training. Additionally, since this dataset is designed for downstream tasks in specific scenarios, some textual instructions include explicit coordinate information. To enhance the generalization ability of the video model, we excluded these coordinate-specific instructions during training.

At the model architecture level, we followed Dynamicrafter (Xing et al., 2023) to modify the text-to-video model of Open-Sora-Plan(T2V) (Lab & etc., 2024) by replacing the first frame and expanding the channel dimensions, enabling the model to take the first frame as a condition. This resulted in the Open-Sora-Plan (TI2V) model. No structural adjustments were made to other models. During training, we preprocessed the data according to each model’s default input format and performed fine-tuning following the official implementation without changing the training settings. We fine-tuned each model using two different video lengths to enhance the diversity of the video evaluation set: short videos with approximately 20 frames and long videos with around 60 frames, depending on the model’s default training video length. The specific lengths are detailed in the Tab. 5.

### B.3 HUMAN PREFERENCE EVALUATOR TRAINING

The Human Preference Evaluator is trained based on Flash-VStream (Zhang et al., 2024a), where only LoRA (Hu et al., 2021) parameters are trained. The model’s input consists of a sampled video, represented as multiple frames, along with a prompt. The prompt includes the current scenario, the instruction input for video generation, the dimension being evaluated, and the definition of that



```
<Video>\n\nThe given autonomous driving video is generated by a generative model based on
the input instruction: {instruction}. Please rate the video based on the following criteria:
{Dimension}: {Dimension Explanation}
```

Figure 6: **Prompt template for Autonomous Driving**. The `{item}` is replaced with specific content.

Table 7: **Evaluation results in OE**. The abbreviations are listed in Tab. 2.

Model	BC	FC	IA	SA	VC	TJ	EI	Overall
Open-Sora-Plan	1.4	1.9	1.7	1.7	<b>2.0</b>	1.5	1.6	1.69
Lavie	1.3	<b>2.0</b>	1.7	1.7	<b>2.0</b>	<b>2.0</b>	<b>1.8</b>	1.79
ModelScope	<b>1.9</b>	<b>2.0</b>	<b>2.0</b>	1.7	<b>2.0</b>	<b>2.0</b>	1.75	<b>1.91</b>
OpenSora	1.6	1.9	1.6	1.8	<b>2.0</b>	<b>2.0</b>	1.6	1.79
AnimateDiff	1.3	1.3	1.2	1.7	1.4	1.38	1.55	1.40
DynamicCrafter	<b>1.9</b>	<b>2.0</b>	1.5	<b>2.0</b>	<b>2.0</b>	<b>2.0</b>	1.45	1.84
EasyAnimate	1.4	1.8	1.5	<b>2.0</b>	<b>2.0</b>	1.22	1.45	1.62

dimension. An example of such a prompt is illustrated in Fig. 6, while the details of the explanation are discussed in Section 2. We don’t use the annotated reason during training for CoT of the evaluator, as the reason labeled by different human varies a lot, hard for model to learn.

We maintain consistent training settings in all three scenarios, with a video sampling frequency of 4. The LoRA settings aligned with those in Flash-VStream. We use AdamW as the optimizer, employ cosine decay for the learning rate scheduler. We train for 4 epochs with a learning rate of  $2e-5$  and a warmup ratio of 0.03. The training is conducted on 4 A100 80 GPUs. To avoid over-fitting to specific prompts or videos generated by particular models, we carefully filter the HF-Embodied Dataset to ensure balanced distribution across various generation models and evaluation dimensions.

We prove the effectiveness and generalizability of through comparison with GPT-4o across the three embodied scenarios, under both finetuned and zero-shot setting, as shown in Tab. 6. After fine-tuning, the Human Preference Evaluator surpasses GPT4-o in aligning with human preferences across all dimensions in every scenario. This is particularly evident in challenging dimensions, *e.g.*, Embodied Interaction and Trajectory in **RM**, where GPT4-o shows a negative correlation, while the Human Preference Evaluator exhibits a strong positive correlation. These results demonstrate the its robust performance, making it suitable for Explicit Perceptual Evaluation. In zero-shot settings, the Human Preference Evaluator also outperforms GPT4-o in nearly all dimensions, further proving our model’s ability to understand videos generated by different models.

## C DETAILED RESULT OF EXPLICIT PERCEPTUAL EVALUATION

### C.1 QUANTITATIVE RESULTS

Tabs. 7-9 present the comprehensive evaluation results for 7 video generation models across three scenarios, including the scores for each dimension and the mean scores representing the overall performance of the models. In **OE**, although our scoring is binary, we display scores on a scale of 1-2 for consistent comparison. In addition to the conclusions mentioned in the main text, we can observe the following findings.

In **OE**, most models achieve high scores in Velocity, largely due to the limited occurrences of object movement in the generated videos. Generating dynamic embodied environments with moving objects presents a significant challenge for current models. Additionally, the consistency between the generated videos and the scenarios specified in the instructions is higher than the alignment with the task-oriented instructions. This indicates that while the models can generate corresponding scenes, they struggle to reason about the temporal actions necessary for task completion.

In **AD**, the quality of the generated videos significantly declines due to the complexity of outdoor driving scenarios. The models must understand and generate various traffic elements, *e.g.*, roads,

Table 8: **Evaluation results in AD.** The abbreviations are listed in Tab. 2.

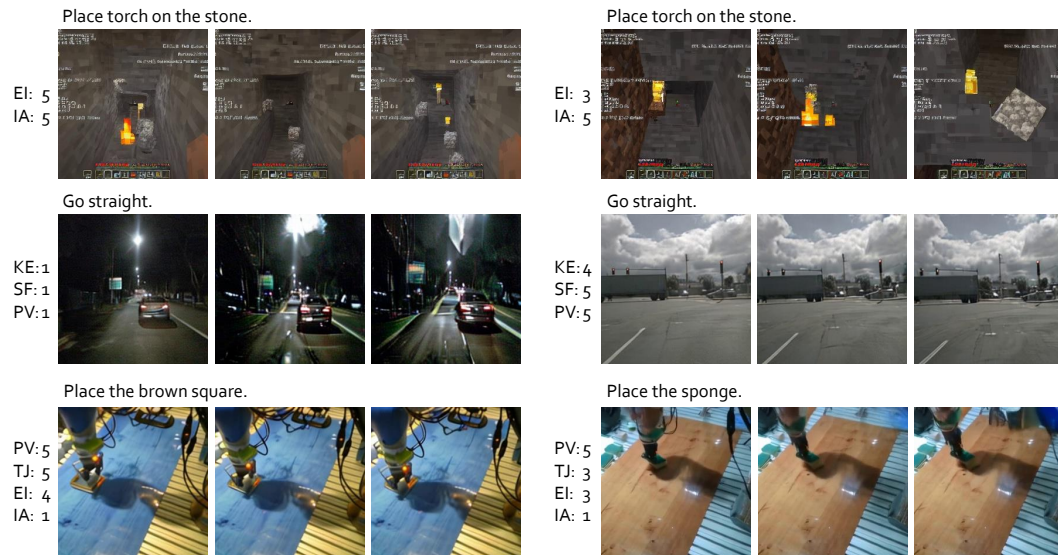
Model	AE	IA	PV	TJ	KE	SF	Overall
Open-Sora-Plan	1.6	<b>5.0</b>	1.55	1.4	1.45	3.2	2.37
Lavie	2.15	<b>5.0</b>	2.2	2.8	2.1	<b>5.0</b>	3.21
ModelScope	2.8	<b>5.0</b>	3.35	4.0	3.0	<b>5.0</b>	3.86
OpenSora	<b>3.55</b>	<b>5.0</b>	<b>4.4</b>	<b>4.8</b>	<b>3.65</b>	<b>5.0</b>	<b>4.40</b>
AnimateDiff	1.55	<b>5.0</b>	1.55	1.0	1.3	3.8	2.37
DynamicCrafter	2.6	4.0	3.4	3.8	2.65	5.0	3.57
EasyAnimate	1.5	3.4	1.4	1.4	1.3	2.6	1.93

Table 9: **Evaluation results in RM.** The abbreviations are listed in Tab. 2.

Model	AE	BC	FC	IA	PV	TJ	EI	Overall
Open-Sora-Plan	<b>4.0</b>	4.0	<b>4.0</b>	1.0	4.9	<b>5.0</b>	4.0	3.84
Lavie	3.8	3.9	<b>4.0</b>	1.8	4.95	<b>5.0</b>	4.1	3.94
ModelScope	3.63	4.1	<b>4.0</b>	1.18	4.9	<b>5.0</b>	4.0	3.83
OpenSora	3.85	4.0	3.95	1.3	4.75	<b>5.0</b>	4.1	3.85
AnimateDiff	3.8	3.9	<b>4.0</b>	1.0	4.95	<b>5.0</b>	4.1	3.82
DynamicCrafter	3.97	<b>4.08</b>	<b>4.0</b>	<b>2.6</b>	<b>5.0</b>	<b>5.0</b>	<b>4.31</b>	4.14
EasyAnimate	3.55	3.45	3.65	1.2	4.8	4.3	3.45	3.49

background buildings, pedestrians, and vehicles, while also producing dynamic content, with each element requiring reasonable speed. This presents substantial challenges. However, top-performing models, *e.g.*, OpenSora, manage to achieve the highest scores across all metrics.

In **RM**, the primary issue lies in Instruction Alignment. The video generation models struggle to comprehend the input instructions and generate appropriate actions to complete the tasks, instead moving aimlessly without clear objectives. This lack of targeted movement reduces potential errors related to object interaction or penetration, resulting in artificially inflated scores in Embodied Interaction and Trajectory. Current video generation models struggle in effectively addressing robotic manipulation tasks.

Figure 7: **Qualitative Results in Explicit Perceptual Evaluation.**

## 1080 C.2 QUALITATIVE RESULTS

1081 We include a qualitative analysis of generated videos under the three embodied scenarios. Each  
1082 video is represented by three evenly sampled frames, with the corresponding generation instructions  
1083 listed above the video. To the left of the videos, we provide the scores of the key embodied attributes  
1084 labeled by the human preference evaluator.

1085 **Open-Ended Embodiment Scenario.** For the open-ended embodiment scenario, the left video  
1086 demonstrates successful completion of the instructed task, with proper interaction with the stone. In  
1087 contrast, the right video encounters issues during interaction, specifically crushing the stone when  
1088 placing the torch, indicating a problematic interaction.

1089 **Autonomous Driving Scenario.** In the autonomous driving context, the left video suffers from sig-  
1090 nificant distortion and light pollution. Additionally, it exhibits unsafe behavior, such as maintaining  
1091 excessive speed despite the presence of a car ahead. On the other hand, the right video maintains  
1092 high-quality generation and demonstrates proper adherence to traffic rules, including slowing down  
1093 at a red light.

1094 **Robotic Manipulation Scenario.** For robotic manipulation, the left video displays that the robotic  
1095 arm interacts with a rigid object (wooden block), which appropriately does not deform during the  
1096 grasping process. However, minor, physically implausible rotations occur during the grasp, resulting  
1097 in a score of 4 for EI. Additionally, the generated wooden block does not match the specified color  
1098 in the instruction, leading to an instruction alignment score of 1. In contrast, the flexible object  
1099 (sponge) in the right video, unrealistically stretched, violating physical rules. Furthermore, the video  
1100 depicts the robotic arm moving away from the table, which contradicts the "place" instruction. This  
1101 mismatch leads to low scores in both trajectory and instruction alignment. Despite these issues, both  
1102 videos effectively display light reflections and shadows, with a clear sense of depth, earning a PV  
1103 score of 5.

1104 These qualitative results provide an illustration of "what is a good embodied video", and reveal the  
1105 limitations of the video generation models.

## 1106 D IMPLICIT MANIPULATIVE EVALUATION-OE

1107 In this section, we provide additional details about Implicit Manipulative Evaluation-**Open-Ended**  
1108 **Embodied Environment** that are not covered in the main paper due to space limitations. Minecraft  
1109 has emerged as a popular open-world environment for developing generalist embodied agents (Lif-  
1110 shitz et al., 2024; Qin et al., 2024; Zhou et al., 2024) due to its diverse tasks (e.g., survival, harvest-  
1111 ing, crafting, combat, and creative tasks), varied environments, and interactive mobs, all of which  
1112 require generalized agent capabilities. Previous works (Qin et al., 2024; Wang et al., 2023d;a) have  
1113 primarily focused on exploring the capabilities of LLMs or MLLMs as Predictive Text Model at the  
1114  $S_1$  stage. However, no prior research has conducted closed-loop evaluations of World Simulators at  
1115 the  $S_3$  stage within Minecraft. To address this gap, we leverage the Steve-1 pipeline to assess the  
1116 performance of Video Generation Models as World Simulators in **Open-Ended Embodied Environ-**  
1117 **ment**.

### 1118 D.1 DETAILED DESCRIPTION

1119 In Implicit Manipulative Evaluation-**Open-Ended Embodied Environment**, we adapt the action space  
1120 of Steve-1 (Lifshitz et al., 2024) to develop a pipeline for the Video Generation Model, enabling it  
1121 to function as a low-level embodied controller. Additionally, we employ Programmatic Evaluation  
1122 to benchmark the low-level embodied control capabilities of the Video Generation Model as World  
1123 Simulators. These tasks are comprehensive, requiring the combination of multiple atomic actions  
1124 and smooth scene transitions. Each aspect rigorously tests the coherence of the generated content,  
1125 the consistency with given instructions, and the model's ability to interact effectively with the envi-  
1126 ronment.

1127 **Testing.** We evaluated performance in **OE** using five tasks: collecting wood, collecting dirt, collect-  
1128 ing seeds, exploring the area, and vertical digging. To reduce evaluation randomness, we selected  
1129 the most suitable initialization environments for each task (e.g., the agent is initialized in a forest  
1130 for the wood collection task). During testing, for each task, we randomly select one description

from various task instructions and input it into the World Simulator to generate the corresponding video. The video is then continuously translated into actions by a pre-trained goal-based video-to-action model, which executes until the test time expires. Each task runs for 10 trials with distinct environment seeds, with a limit of 3,000 frames (*i.e.*, 2.5 minutes of gameplay).

**Training.** Due to the low video quality produced by the open-source video generation model based on the provided instructions, we applied additional fine-tuning using data from the **OE** simulation environment. For Video Generation Model fine-tuning, we use OpenAI Contractor Gameplay Dataset (Baker et al., 2022) which is the same as **OE** in Explicit Perceptual Evaluation. The training setting could be found in Sup. B.2. For pre-trained goal-based video-to-action model, we use pre-trained Steve-1(visual) model without extra fine-tuning.

**Metrics.** We calculate programmatic evaluation metrics by tracking the MineRL environment state throughout each evaluation episode. Several metrics are measured, including travel distance and early-game item collection. Travel distance is defined as the agent’s maximum displacement on the horizontal (X-Z) plane from its initial spawn point. Dig depth is defined as the agent’s maximum displacement on the vertical (Y) axis from its initial spawn point. For an early-game inventory, we record the maximum count of logs, seeds, and dirt items observed in the agent’s inventory during the episode.

## D.2 ACTIONS

We use the part of the action space of (Baker et al., 2022) which encompasses nearly all actions available to human players, including keypresses, mouse movements, and clicks. The specific binary actions used in our setup are listed in Tab 10.

Table 10: Action Space of **OE**.

Behavior	Action
forward	W key
back	S key
left	A key
right	D key
jump	space key
inventory	E key
sneak	shift key
sprint	ctrl key
attack	left mouse button

## D.3 FULL RESULT

Tab. 11 presents the evaluation results of several models across five specific tasks (collect wood, collect dirt, collect seeds, travel distance, and dig depth), along with the average (AVG) score for each model. The models are evaluated under two different conditions: Text and Text & Image. Notably, to ensure that each task falls within a similar score range, we divided the score for the travel distance task by 10 to calculate the AVG score.

**Performance of Models Under Text Condition.** Open-Sora-Plan and Lavie demonstrate strong performance under the text-only condition, especially in the collect dirt and travel distance tasks. Their average scores (26.38 and 26.06, respectively) are very close, indicating consistent and robust performance across tasks. ModelScope shows an excellent score in the collect dirt task (52.20), but it performs poorly in tasks like collect wood (14.00) and travel distance (240.72), resulting in an overall lower average score (21.050) compared to other text-based models. OpenSora stands out with the highest overall average score (27.80), excelling particularly in collect dirt (70.20) and travel distance (339.87). This suggests that it is well-adapted to a variety of tasks and exhibits strong task performance. AnimateDiff shows the weakest performance across all tasks, especially in collect wood (7.40) and collect seeds (3.30), indicating challenges in handling such tasks.



**Performance of Models Under Text & Image Condition.** Open-Sora-Plan shows a significant drop in average score under the "Text & Image" condition, demonstrating that adding image input reduces its performance compared to the text-only condition. In particular, its travel distance score drops from 342.91 to 195.14, suggesting that incorporating image data might interfere with certain tasks. DynamiCrafter and EasyAnimate exhibit poor performance across all tasks, especially in collect wood and collect seeds, where they barely complete the tasks (with scores of 0.40 and 0.20, respectively). This may indicate a lack of generalization ability in these models when combining image input with text. Comparing the "Text" and "Text & Image" conditions, we observe that adding image input does not consistently improve task performance and, in some cases, even degrades it. We also observed that the success rates of various tasks significantly decrease when an image is added as an additional condition. This indicates that the current video generation models need improvement in handling multiple conditional inputs.

Table 11: Detail Result of **Open-Ended Embodied Environment** in Implicit Manipulative Evaluation.

Model	Condition	AVG	Specific Tasks				
			Collect Wood	Collect Dirt	Collect Seed	Travel Dis.	Dig Depth
Open-Sora-Plan	Text	26.38	19.90	50.20	7.30	342.91	20.20
Lavie		26.06	23.50	56.00	11.60	270.20	12.20
ModelScope		21.050	14.00	52.20	6.30	240.72	8.70
OpenSora		27.80	21.20	70.20	10.40	339.87	3.20
AnimateDiff		13.10	7.40	22.90	3.30	274.19	4.50
Open-Sora-Plan	Text & Image	10.28	11.10	12.50	2.60	195.14	5.70
DynamiCrafter		4.06	0.40	0.30	1.30	130.04	5.30
EasyAnimate		4.84	0.20	0.70	1.70	157.12	5.90

#### D.4 ROLL OUT

Fig. 8 illustrates the downstream execution process in the **Open-Ended Embodied Environment**, along with the corresponding textual instructions.



Figure 8: Rollout of **Open-Ended Embodied Environment** in Implicit Manipulative Evaluation.

## E IMPLICIT MANIPULATIVE EVALUATION-AD

In this section, we provide additional details about Implicit Manipulative Evaluation-**Autonomous Driving** that are not covered in the main paper due to space limitations.



## E.1 DETAILED DESCRIPTION

In Implicit Manipulative Evaluation-**Autonomous Driving**, we adapt the action space of LM-Drive (Shao et al., 2024) to develop a pipeline for the Video Generation Model, enabling it to function as a low-level embodied controller. Additionally, we employ LangAuto (Language-guided Autonomous Driving) CARLA benchmark, to evaluate the low-level embodied control capabilities of the Video Generation Model as World Simulators. These tasks are designed to be comprehensive, spanning all 8 publicly available towns in CARLA, covering a diverse range of scenarios *e.g.*, highways, intersections, and roundabouts. Additionally, they account for 16 different environmental conditions, combining 7 distinct weather settings (Clear, Cloudy, Wet, MidRain, WetCloudy, HardRain, SoftRain) with 3 daylight conditions (Night, Noon, Sunset). Each aspect rigorously tests the coherence of the generated content, the consistency with given instructions, and the model’s ability to interact effectively with the environment.

**Testing.** We evaluated performance in **Autonomous Driving** using the LangAuto-Tiny benchmark setting where the route length is shorter than 150 meters. We posit that shorter driving distances provide a more effective test of the low-level control capabilities of World Simulators. Longer routes typically involve more instructions, which are prone to misalignment with the real-time simulation environment. Therefore, we opt to evaluate performance on shorter routes to minimize these discrepancies. During testing, we randomly select one description from various task instructions and input it into the World Simulator to generate the corresponding video. The video is then continuously translated into actions by a pre-trained goal-based video-to-action model, which executes until the test time expires. We use the corresponding LangAuto-Tiny instructions and the first-person view rendered by the real-time CARLA simulation environment as input to the video generation model. The generated video is then continuously transformed into downstream control signals using a pre-trained video-to-action model until the agent reaches a predefined success zone or the task is terminated due to factors *e.g.*, timeouts or collisions.

**Training.** Due to the low video quality produced by the open-source video generation model based on the provided instructions, we applied additional fine-tuning using data from the **AD** simulation environment. For Video Generation Model training, we use LMDrive Training Dataset (Shao et al., 2024). We preprocessed the training data according to each model’s default input format and performed fine-tuning following the official implementation without changing the training settings. We fine-tuned each model using a short video generation setting with approximately 20 frames. For the video-to-action model, we use pre-trained LMdrive model. Additional fine-tuning was conducted based on the test requirements. We provided the model with arbitrary text instructions and replaced the visual input with the future frame while keeping all other training settings consistent with LM-Drive.

**Metrics.** We consider eight key metrics introduced by the CARLA Leaderboard (Dosovitskiy et al., 2017): Route Completion (RC), Infraction Score (IS), Driving Score (DS), Vehicle Collisions (VC), Pedestrian Collisions (PC), Layout Collisions (LC), Red Light Violations (RV), and Offroad Infractions (OI). Route Completion refers to the percentage of the total route length that the agent has completed. This metric only accounts for the distance traveled along the predetermined route, where each segment corresponds to a navigation instruction. If the agent strays too far from the route, it is considered to have violated the instruction, resulting in the episode being marked as a failure and terminated. The Infraction Score tracks any infractions caused by the agent, with penalties applied for collisions or traffic violations through a corresponding discount factor. The Driving Score is the product of the route completion ratio and the infraction score, reflecting both driving progress and safety, and is widely regarded as the primary ranking metric. The precise definitions of the residual metrics can be found in the CARLA documentation (Dosovitskiy et al., 2017).

## E.2 ACTIONS

The video generated by the World Simulator is continuously fed into the video-to-action model to obtain the corresponding waypoints. The agent then generates control signals based on the generated waypoints and the conversion strategy used in CARLA.

### E.3 FULL RESULT

Tab. 12 presents the evaluation results of several models across eight metrics. The evaluation results highlight significant differences in how video generation models perform in autonomous driving tasks. Open-Sora-Plan stands out in trajectory generation, instruction following, and environment perception, producing high-quality videos that effectively support task execution. In contrast, DynamiCrafter and EasyAnimate struggle with generating detailed and consistent video content, particularly when handling complex or dynamic scenes. These models require improvements in video generation quality, scene understanding, and task alignment to enhance their performance.

From a video generation perspective, several key areas for future development are identified: Improved Trajectory Generation: High-quality trajectory generation is essential for accurate control signals. Models must focus on generating more coherent and precise trajectories, especially in dynamic environments, to ensure vehicles follow instructions and avoid collisions. Enhanced Instruction Following: Generated videos should closely align with task instructions, particularly in changing environments, enabling vehicles to adapt quickly while maintaining task accuracy. Better Environment Perception: Future models need to generate videos that accurately represent complex scenes, *e.g.*, interactions with pedestrians, other vehicles, and varied terrains. More detailed and realistic video generation will provide stronger input for real-time decision-making in the control system.

In summary, advancing trajectory accuracy, instruction alignment, and environment representation will be crucial for improving the overall performance of these video generation models in autonomous driving tasks.

Table 12: Detail Result of **Autonomous Driving** in Implicit Manipulative Evaluation.

Model	DS(↑)	RC(↑)	IS(↑)	VC(↓)	PC(↓)	LC(↓)	RV(↓)	OI(↓)
Open-Sora-Plan	31.054	38.249	0.767	2.400	0.000	4.401	1.133	3.514
DynamiCrafter	24.491	37.189	0.599	5.030	0.000	4.896	0.937	3.221
EasyAnimate	17.414	28.475	0.607	0.000	0.000	29.344	0.000	1.690

### E.4 ROLL OUT

Fig. 9 illustrates the downstream execution process in the **Autonomous Driving**, the corresponding text instructions can be found in the lower left corner of each frame.

## F IMPLICIT MANIPULATIVE EVALUATION-RM

In this section, we provide additional details about Implicit Manipulative Evaluation-**Robot Manipulation** that are not covered in the main paper due to space limitations.

### F.1 DETAILED DESCRIPTION

We primarily conduct our experiments on the CALVIN benchmark (Mees et al., 2022), which is specifically designed for long-horizon, language-conditioned manipulation tasks. CALVIN includes four simulated environments (labeled A, B, C, and D) that differ in textures and object placements. Each environment features a Franka Emika Panda robot positioned next to a desk with various manipulable objects. The evaluation protocol tests model performance across 1,000 unique instruction chains, each consisting of five distinct tasks. By providing an extensive dataset paired with natural language annotations, the CALVIN benchmark can provide a close-loop evaluation platform for evaluating World Simulator to test its generation and generalization capabilities.

**Testing.** We evaluated performance in **Robot Manipulation** using the CALVIN benchmark benchmark, policy models are trained on demonstrations from environments A, B, and C, and evaluated in a zero-shot manner in environment D. During the testing phase, we leverage World Simulators and a pre-trained video-to-action model to tackle novel manipulation tasks guided by user-specified natural language commands. Given a current observation, we generate future video predictions using

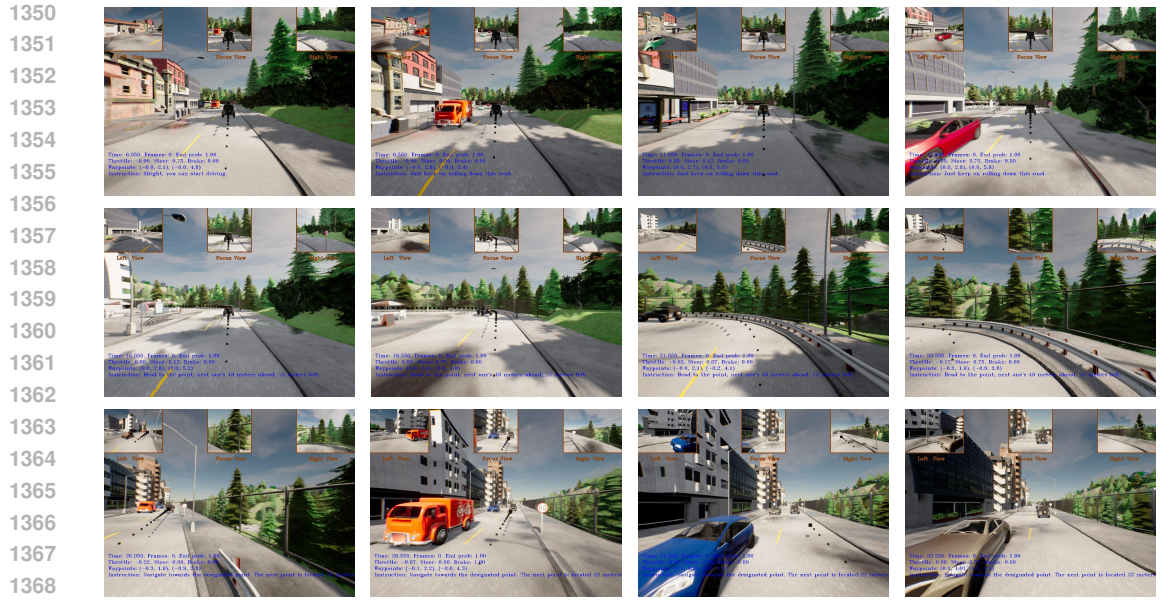


Figure 9: Rollout of Autonomous Driving in Implicit Manipulative Evaluation.

the World Simulator for the manipulation task with text instruction. Once the video is sampled, we then execute the video-to-action policy conditioned on for  $k$  timesteps, where  $k$  is a testing hyperparameter. After  $k$  timesteps, the video prediction is refreshed by sampling from the World Simulator again, and the process is repeated.

**Training.** Due to the low video quality produced by the open-source video generation model based on the provided instructions, we applied additional fine-tuning using data from the RM simulation environment. For Video Generation Model training, we use Calvin(ABC\_D) dataset (Mees et al., 2022). We preprocessed the training data according to each model’s default input format and performed fine-tuning following the official implementation without changing the training settings. We fine-tuned each model using a short video generation setting with approximately 20 frames. For the video-to-action model, we use a pre-trained Susie policy without extra fine-tuning.

**Metrics.** We report the success rates and the average task length completed (out of five tasks) for each evaluation sequence.

## F.2 ACTIONS

For low-level control, we utilize the same action space as Calvin (Mees et al., 2022).

## F.3 FULL RESULT

Based on the results shown in Tab. 13, Open-Sora-Plan demonstrates consistent performance, with an average task length of 2.95, indicating its ability to reliably complete task sequences. While DynamicCrafter achieves a higher success rate of 0.95 on the initial task, its performance declines as task complexity increases, suggesting limitations in handling longer manipulation sequences. EasyAnimate, although moderately successful in completing early tasks, experiences a sharp decline in performance as task difficulty rises, reflected in its lower average task length of 2.05.

Overall, the models’ ability to consistently complete multiple tasks in succession showcases their potential in downstream applications, with Open-Sora-Plan emerging as the most capable. However, the observed decrease in success rates as task complexity increases highlights the need for further improvements in video-to-action translation, particularly in addressing the challenges posed by longer and more complex manipulation sequences.

Table 13: Detail Result of **Robot Manipulation** in Implicit Manipulative Evaluation.

Method	Task completed in a row (%) $\uparrow$					Avg. Len. $\uparrow$
	1	2	3	4	5	
Open-Sora-Plan	0.85	0.70	0.60	0.40	0.40	2.95
DynamiCrafter	0.95	0.75	0.55	0.25	0.25	2.75
EasyAnimate	0.90	0.60	0.35	0.10	0.10	2.05

To minimize the impact of randomness caused by the number of experiments, we conducted an additional 100 trajectories evaluation. The results are presented in Tab 14. Compared to the 20-trajectories setup, the results from the 100-trajectories setup show slight variations but maintain a consistent overall trend. We also compared the performance with Unipi based on the 25-trajectory setup described in SuSIE, and it can be observed that the tested video generation models(Open-Sora-Plan, DynamiCrafter, EasyAnimate) demonstrate superior capabilities compared to the PVDM Yu et al. (2023) latent video diffusion model utilized by Unipi.

Table 14: Detail Result of **Robot Manipulation** in Implicit Manipulative Evaluation, by running 100 trajectories. \* Results reported by Susie Black et al. (2023).

Method	Task completed in a row (%) $\uparrow$					Avg. Len. $\uparrow$
	1	2	3	4	5	
UniPi* (HiP)	0.08	0.04	0.00	0.00	0.00	-
UniPi* (Susie)	0.56	0.16	0.08	0.08	0.04	-
Open-Sora-Plan	0.89	0.72	0.63	0.34	0.32	3.12
DynamiCrafter	0.93	0.69	0.51	0.27	0.18	2.64
EasyAnimate	0.92	0.55	0.32	0.16	0.13	2.08

#### F.4 ROLL OUT

Fig. 10 illustrates the downstream execution process in the **Robot Manipulation**, along with the corresponding textual instructions.

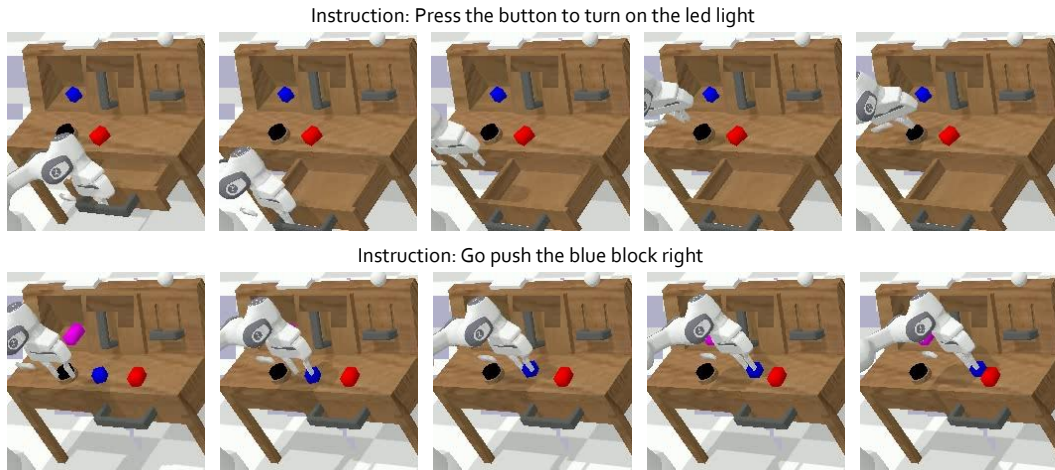


Figure 10: Rollout of **Robot Manipulation** in Implicit Manipulative Evaluation.

## G DISCUSSION OF VISION-LANGUAGE-ACTION MODELS

The generated videos have the potential to significantly enhance the performance of Vision-Language-Action (VLA) models by addressing two key challenges in training such models: the



1458 availability of diverse, high-quality training data and the need for effective reward functions in real-  
1459 world scenarios.

1460 **Data Augmentation and Hindsight Relabeling for Imitation Learning.** Generated videos can  
1461 serve as a valuable source of synthetic data for training VLA models. By leveraging the diversity  
1462 and scalability of generative models, we can create a wide array of training scenarios, covering  
1463 edge cases and rare events that are difficult to capture in real-world datasets. Additionally, these  
1464 videos enable hindsight relabeling, a process where we retrospectively adjust the labels of generated  
1465 data to align with desired outcomes. This approach is particularly effective for imitation learning,  
1466 allowing VLA models to learn optimal behavior by mimicking successful trajectories represented  
1467 in the generated videos. By expanding the data distribution and improving its quality, generative  
1468 videos can lead to more robust and generalizable VLA models.

1469 **Reward Generation for Online Reinforcement Learning.** Beyond data augmentation, generated  
1470 videos can act as a Reward Generator in reinforcement learning (RL) contexts. Unlike traditional  
1471 RL setups that rely on pre-defined reward functions within a simulator, generative videos enable the  
1472 creation of dense and context-aware reward signals tailored to real-world tasks. For example, they  
1473 can simulate desirable outcomes or intermediate goals, providing detailed feedback to the agent.  
1474 This capability is particularly crucial for transferring RL models to real-world environments, where  
1475 designing explicit reward functions is often impractical. By aligning the generated rewards with  
1476 real-world objectives, we can bridge the gap between simulation and reality, allowing VLA models  
1477 to achieve higher performance in real-world tasks.

1478  
1479  
1480  
1481  
1482  
1483  
1484  
1485  
1486  
1487  
1488  
1489  
1490  
1491  
1492  
1493  
1494  
1495  
1496  
1497  
1498  
1499  
1500  
1501  
1502  
1503  
1504  
1505  
1506  
1507  
1508  
1509  
1510  
1511